

Field Guide to the Minnelusa Formation Ranch A and Newcastle Area, Wyoming and South Dakota

S.G. Fryberger, N. Jones and M. B. Johnson
Enhanced Oil Recovery Institute, University of Wyoming
Laramie, Wyoming
2014

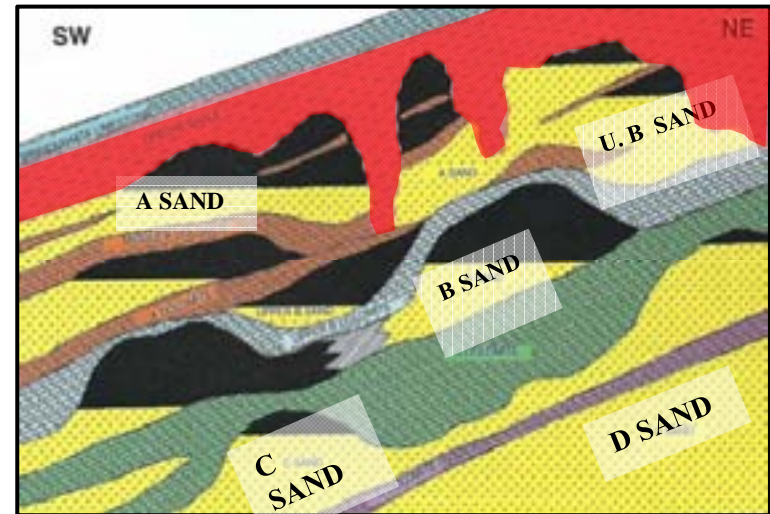


The Middle and Upper Minnelusa Formation at Ranch A, Wyoming

Field Guide to the Minnelusa Formation

Contents

1. Purpose of field trip	<i>page 3</i>
2. Trip Overview	<i>page 4</i>
3. Ranch A	<i>page 8</i>
4. Sand Creek South	<i>page 12</i>
5. Redbird Canyon	<i>page 15</i>
6. Hell Canyon, South Dakota	<i>page 28</i>
7. Minnelusa Regional Geology	<i>page 31</i>
8. Modern and Ancient Analogues	<i>page 44</i>
9. References Cited and Bibliography	<i>page 63</i>
10. Notes and sketch pages	<i>page 66</i>



Minnelusa hydrocarbon trapping configurations

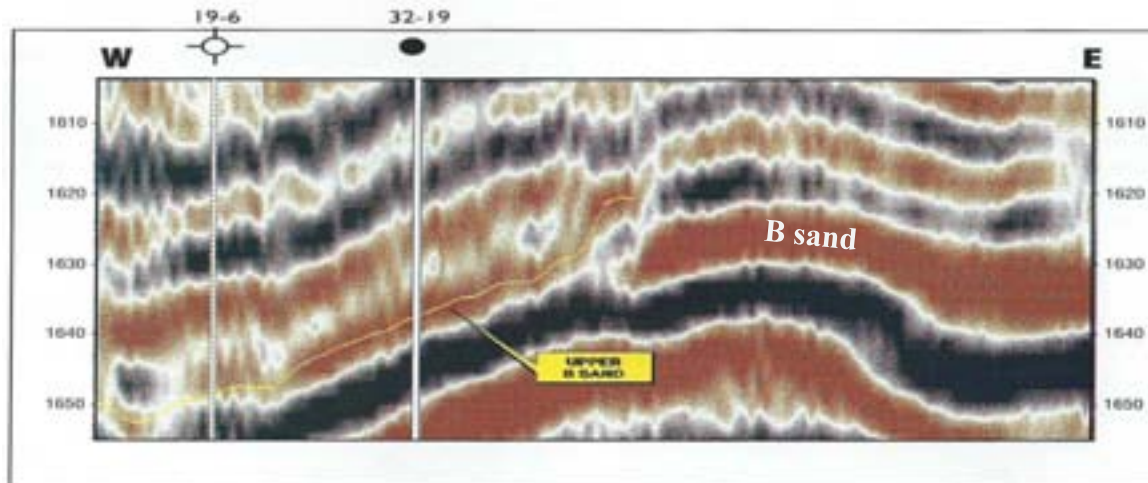
This document is Copyright 2014, by Steven Fryberger Petroleum LLC and Enhanced Oil Recovery Institute, University of Wyoming. All rights reserved.

1. Purpose of Field Trip

The purpose of this field trip and the lectures is to acquaint participants with the sedimentology of the Middle and Upper Minnelusa Formation, using outcrops in the Black Hills of Wyoming and South Dakota. The trip provides a good opportunity to examine in outcrop many of the sedimentary facies that strongly control oil production in the nearby Minnelusa oil play. Along with study of the outcrops, we review important principles of oil and gas production from eolian reservoirs using modern and ancient oil field and outcrop examples. These ideas may be useful in analyzing eolian reservoirs for secondary or tertiary recovery operations, or understanding past reservoir behavior.

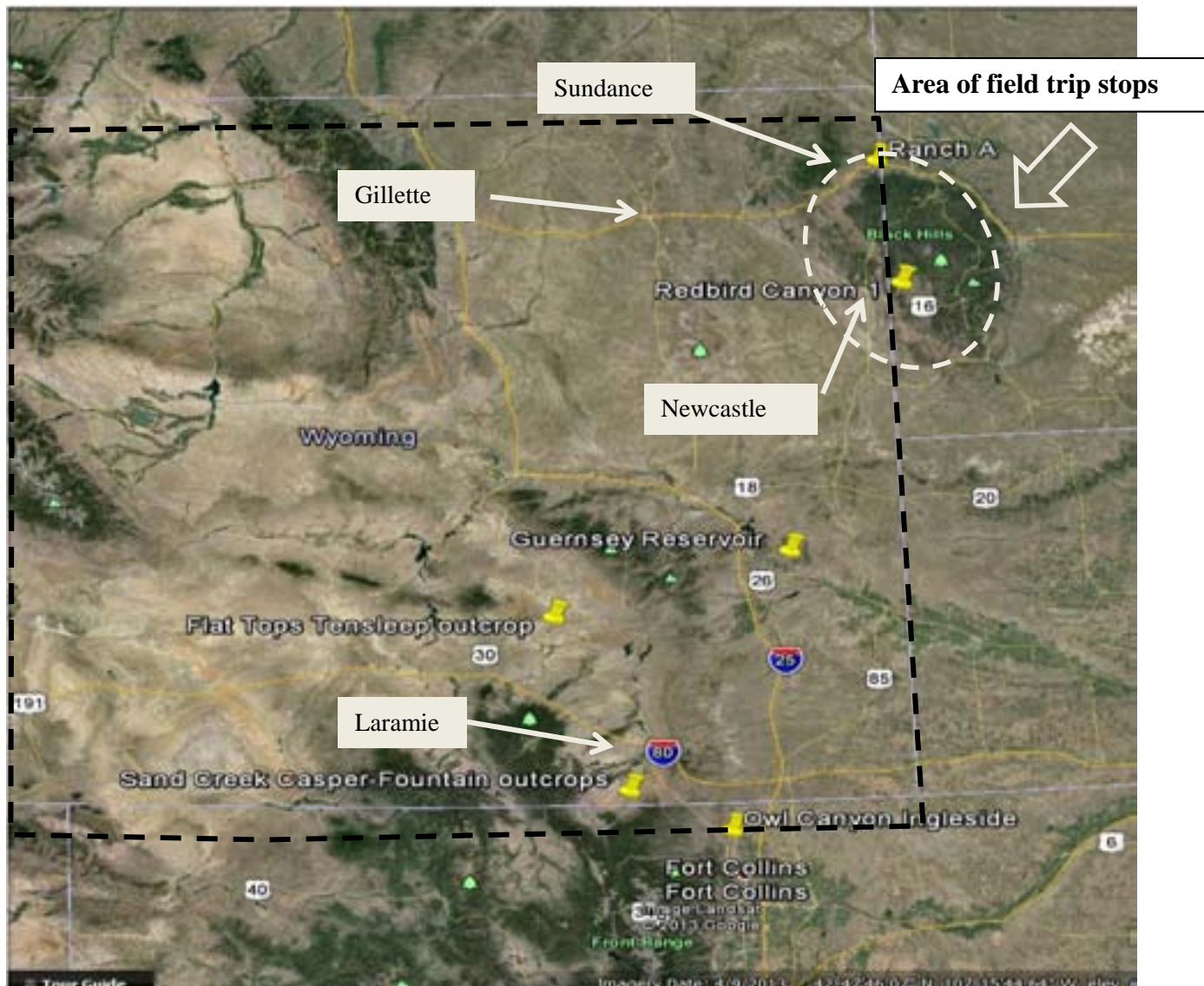
Eolian petroleum reservoirs are found worldwide, many having high-volume production of both oil and gas. As with any geological rock unit, each oil/gas field has production characteristics peculiar to its geological history. However, certain common factors link most eolian reservoirs. Cross-stratification due to bedform migration can influence sweep direction and efficiency. The various kinds of primary eolian strata have different poroperm characteristics. Moreover, stacking of sand seas or bedforms through geological time can create distinctive reservoir flow units in the subsurface. Tectonic activity, especially faults, may create shear zones with reduced poroperm, or partition a reservoir into structurally defined flow units. Faults may also create high-permeability zones that allow water breakthrough. Eolian reservoirs are commonly thought of as clean, and rather simple. However, in some places they are complex in terms grain composition or texture. They are commonly cemented by carbonates, anhydrites or salt, which sets up fabric-selective or non-fabric selective patterns of secondary porosity in reservoirs.

We hope you enjoy and learn from this trip. The subject of eolian reservoirs is too extensive to cover in the two days of this excursion, but we will attempt to hit the high points! Meanwhile, always be safe, don't climb onto exposed places, look out below you for others and use sun protection.



High resolution seismic line at North Donkey Creek Field, showing an Upper B sand preserved in accommodation space where the underlying B Sand has thinned. This principle operates worldwide in eolian deposits. After Frederick, Dean, Fryberger and Wilcox, 1995

2. Trip Overview: *Field trip localities in the Black Hills, Wyoming and South Dakota* *Regional overview Google Earth*

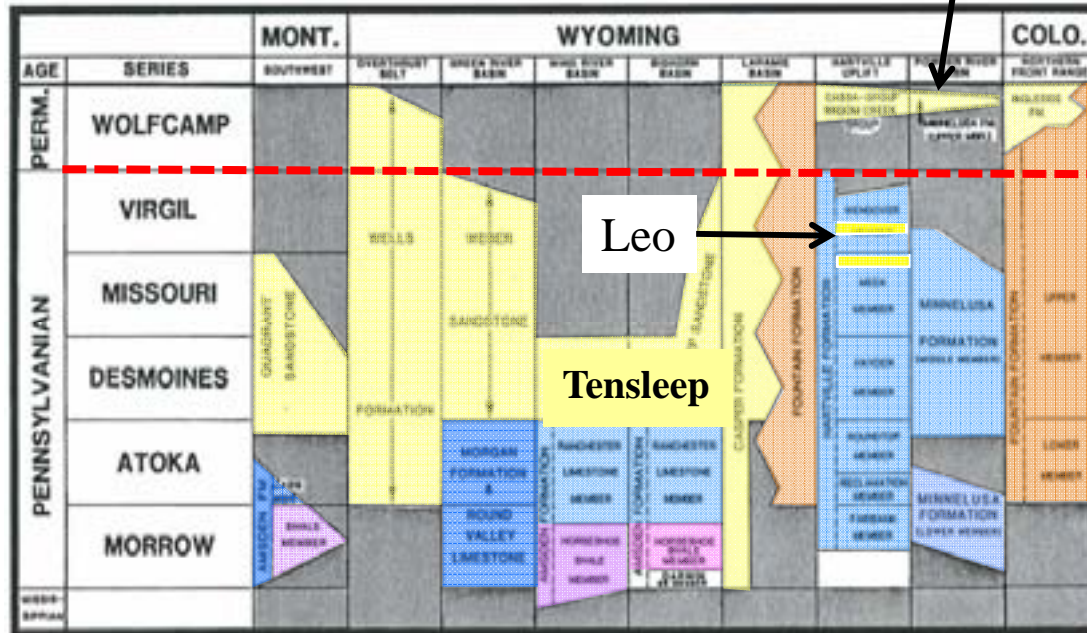


Courtesy of Google Earth

Fryberger, Jones and Johnson, 2014

2. Trip overview: *Minnelusa/Tensleep Formations stratigraphy*

Permo-Pennsylvanian Rocks of the Northern Rockies



After Inden, et al, 1996

Tensleep schematic cross section Southern Wyoming

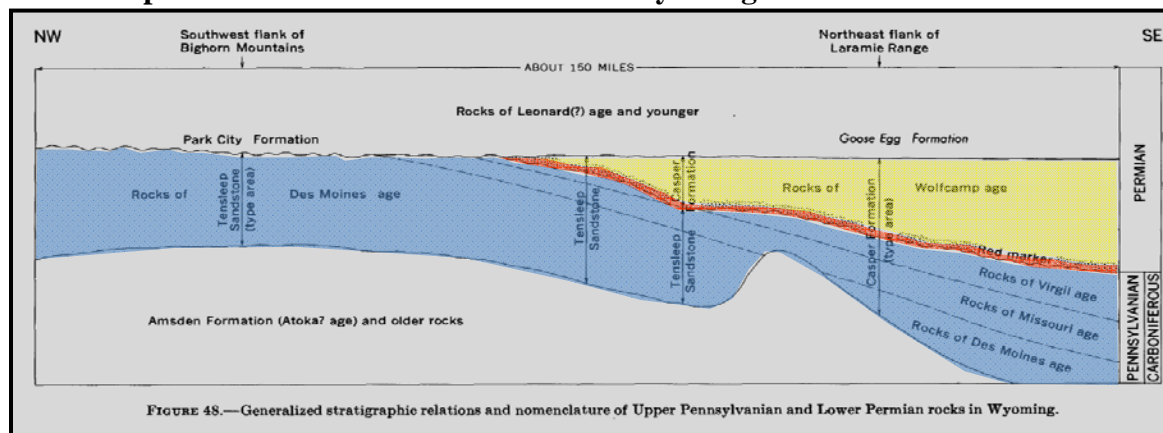


FIGURE 48.—Generalized stratigraphic relations and nomenclature of Upper Pennsylvanian and Lower Permian rocks in Wyoming.

After McKee et al, 1967

2. Trip Overview: Lower Permian (Wolfcampian) isopachs around the Black Hills

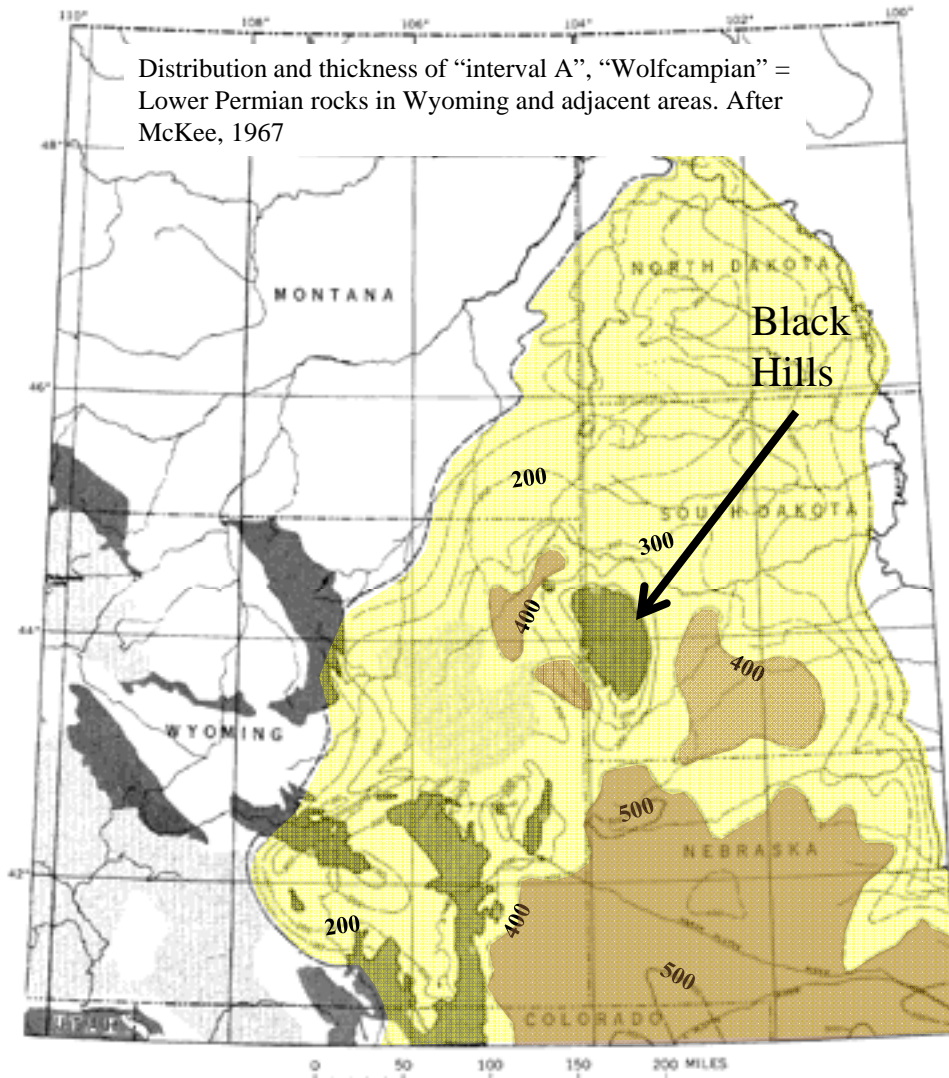
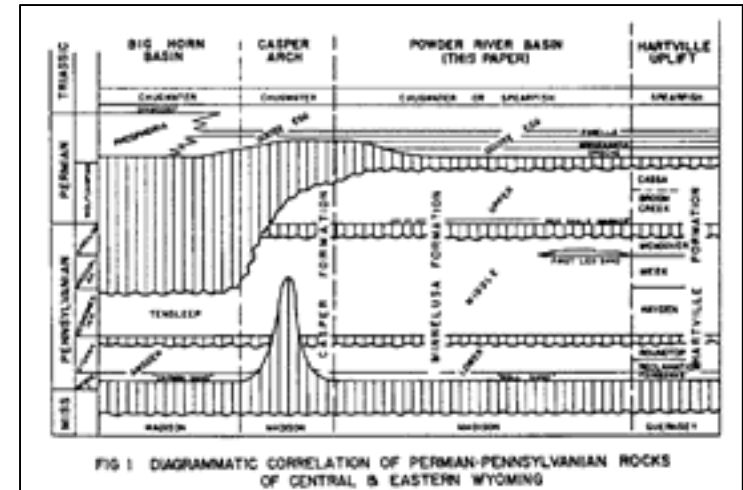


FIGURE 46.—Thickness of interval A in central Wyoming, eastern Montana, the Dakotas and parts of adjacent States discussed in this chapter. Isopach intervals 100 and 500 feet. Isopachs dashed where control is poor, dotted where Permian rocks have not been penetrated by drill. Dark pattern, areas where rocks older than Permian are exposed; light pattern, areas where rocks younger than interval A have not been penetrated.

Fryberger, Jones and Johnson, 2014



Regional unconformities in the Permo-Pennsylvanian rocks of Wyoming. After Foster, 1958

- Interval A of Paleotectonic maps
- Interval B of Paleotectonic maps

TABLE 2.—Subdivisions of the Hartville Formation proposed by Condra, Reed, and Scherer (1940) and their approximate ages (Loe and others, 1955; Agaton, 1954; Foster, D. I., 1958)

Division	Group	Approximate age	System
I	Casa	Leonard	Permian
	Broom Creek	Wolfcamp	
II	Wendover	Virgil	Pennsylvanian
	Meek	Missouri	
III	Hayden	Des Moines	
IV	Round Top		
V	Reclamation	Atoka	
VI	Fairbank	Morrow(?)	

Hartville "Formation"

Subdivisions of the Hartville Formation, SE Wyoming. After McKee et al, 1967

3. Ranch A: *Middle and Upper Minnelusa outcrops*



The Middle Minnelusa outcrops are well preserved. Upper Minnelusa outcrops have experienced solution collapse of evaporites, although the sedimentology is still well preserved.

3. Ranch A: Middle and Upper Minnelusa outcrop



Ranch A Minnelusa outcrop. Lower slope with black shales is Middle Minnelusa. Upper slope with trees and collapsed sands is the Upper Minnelusa. Assignment of Middle clifty sands, the “Upper Red Zone” of the measured section is uncertain in assignment.,



Pahasapa Fm. limestone in Sand Canyon. It is very fossiliferous with many broken shells and crinoid stem fragments.

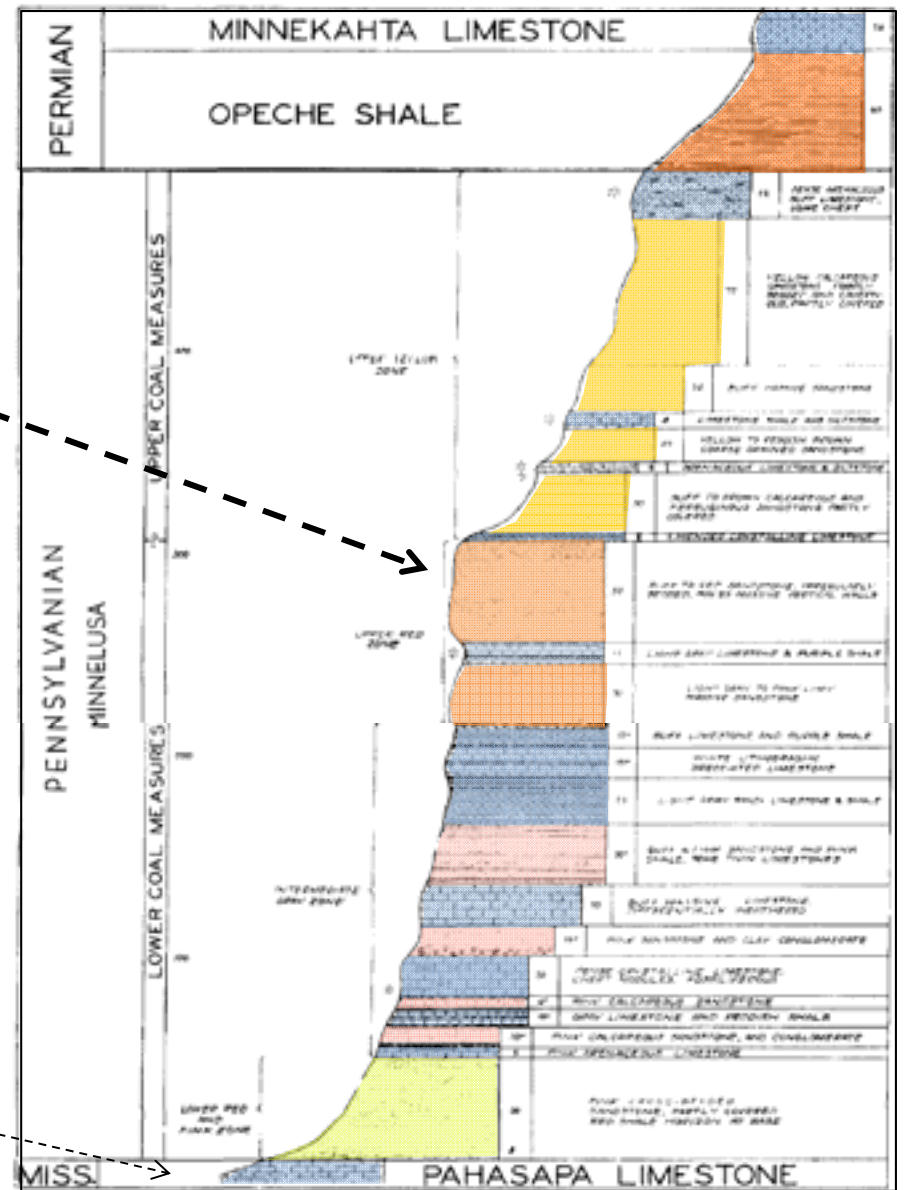
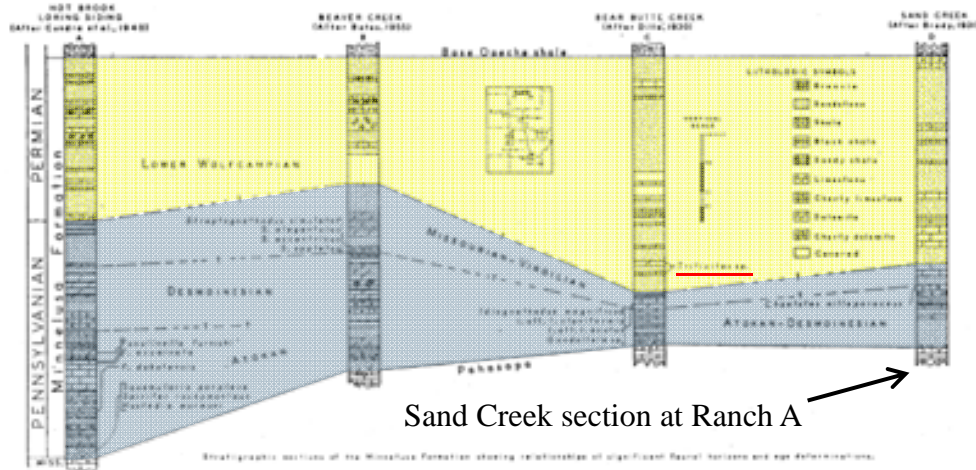
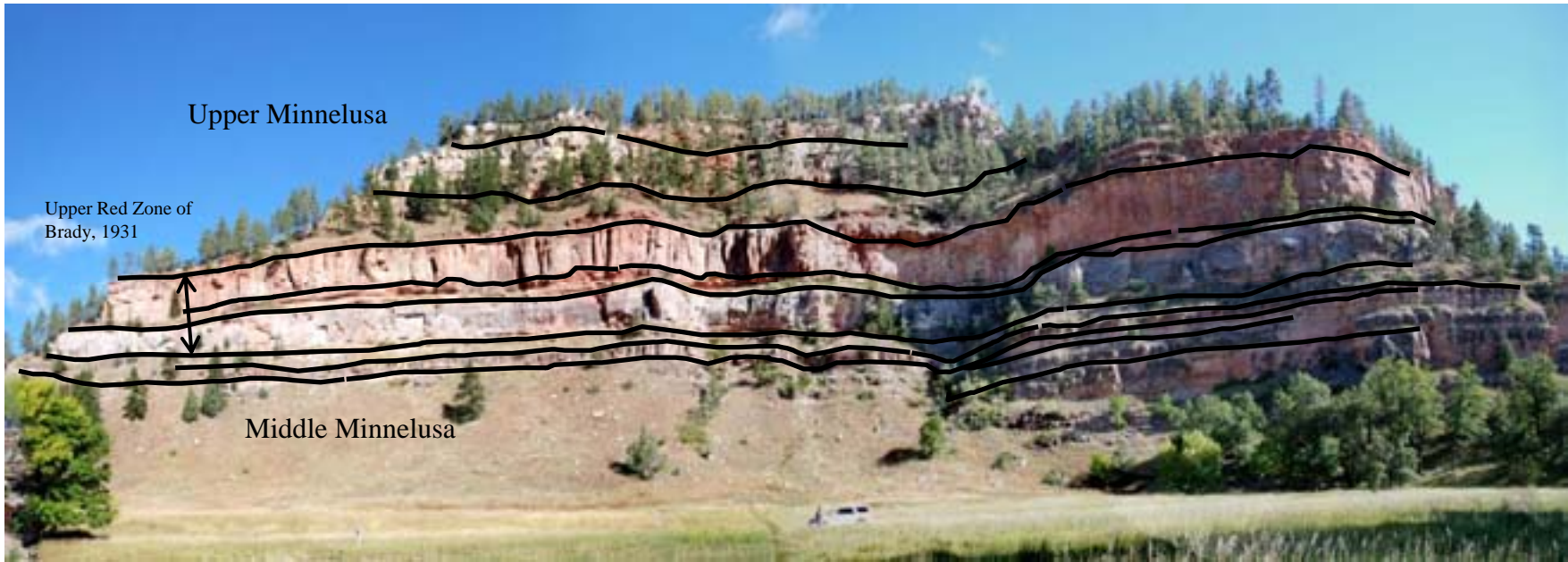


FIG. 1.—Generalized columnar section of Minnekahta, Opeche, and Minnelusa formations at La Plant Ranch in Sand Creek Canyon, south of Beulah, Wyoming, showing age, four lithological zones, and fossiliferous horizons (*) of Minnelusa formation of northwestern Black Hills.

Measured section in the Minnelusa at Ranch A. After Brady, 1931

3. Ranch A: *Bounding surface sketch*



Cross section of Minnelusa near Beulah

Sand Creek section at Ranch A

TEXT-FIG. 1—Stratigraphic sections of the Minnelusa Formation showing relationships of significant faunal horizons and age determinations.

After Jennings, 1959

Fryberger, Jones and Johnson, 2014

- Permian
- Pennsylvanian

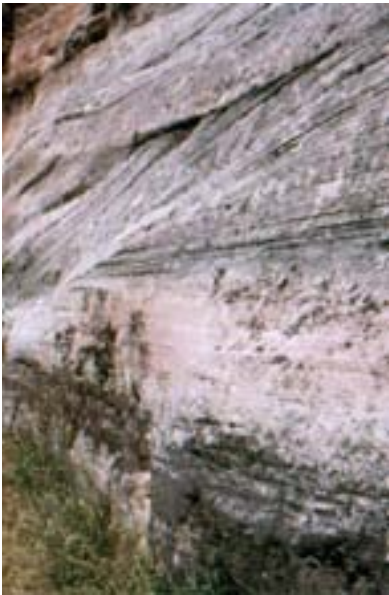
3. Ranch A: *Eolian dune and sabkha bedding in Upper Minnelusa*



Upper Minnelusa Formation medium scale genetic units.



Google Earth view of outcrop. View is to north.



Eolian cross lamination



Eolian sabkha bedding



Eolian ripple and avalanche strata, mostly cross-bedded.



Recessed weathering along clay rich interdune

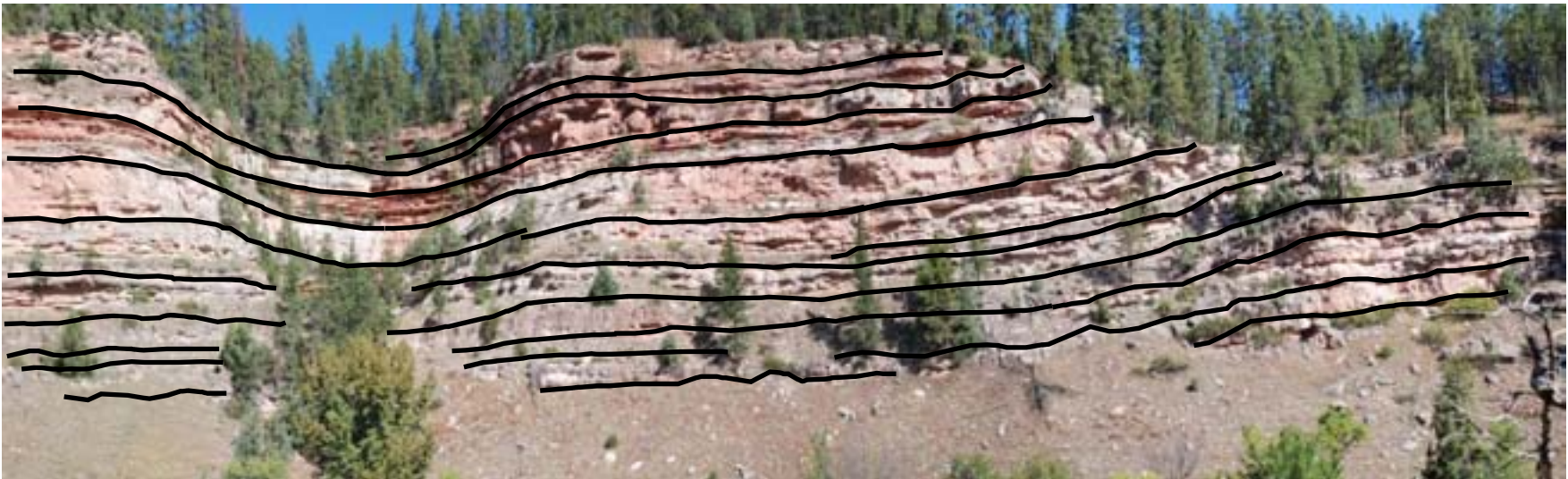
4. Sand Creek South: *Middle and Upper Minnelusa outcrop*



4. Sand Creek South: *Middle and Upper Minnelusa outcrop*



Bounding surface analysis



4. Sand Creek South: *Middle Minnelusa* outcrop detail views



Eolian cross strata (mostly avalanche) , Middle Minnelusa



Outcrop weathering profile, upper part of Middle Minnelusa



Crossbedded fossiliferous dolomite, Middle Minnelusa, outcrop view

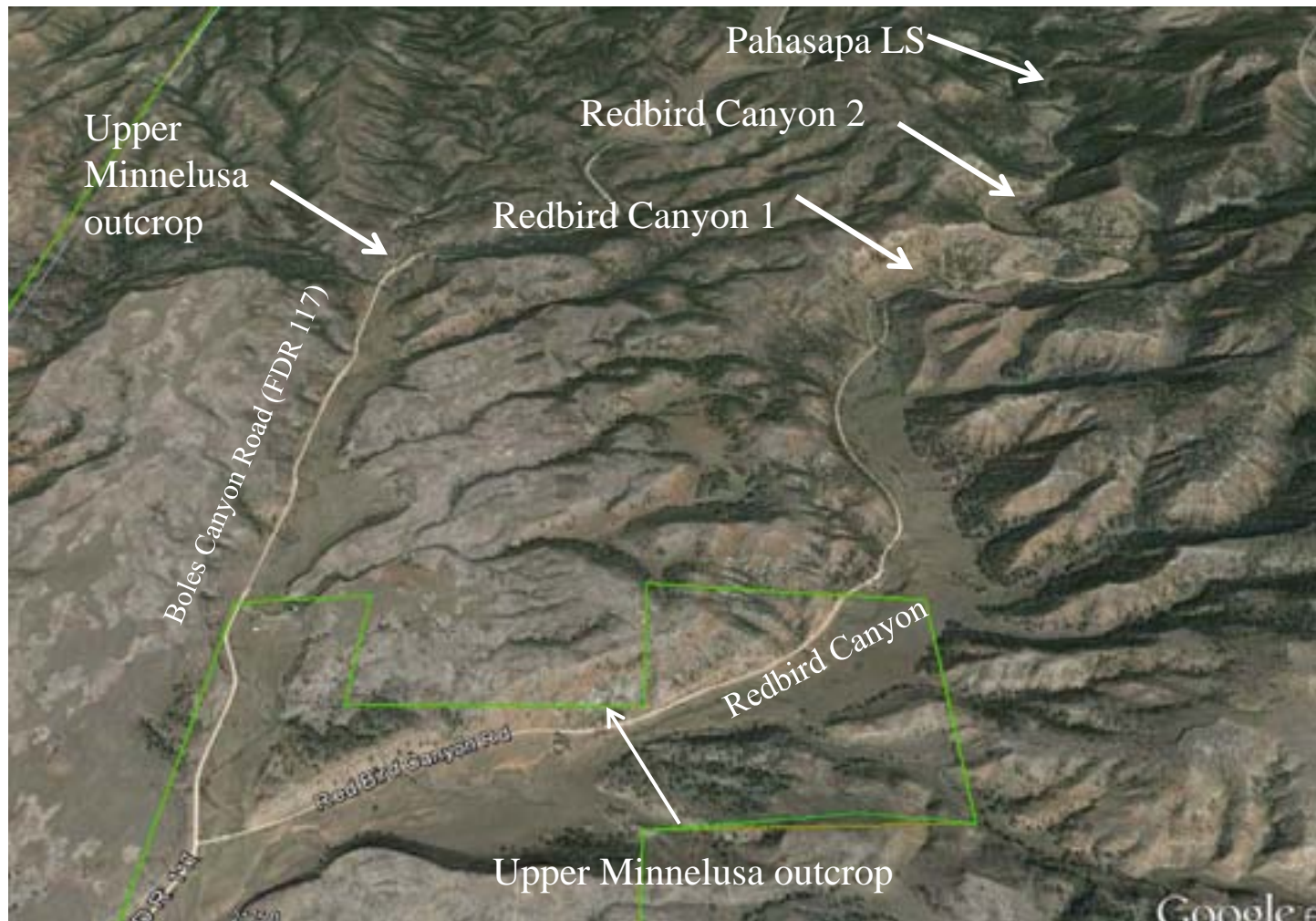


Inverse-graded strata in Middle Minnelusa

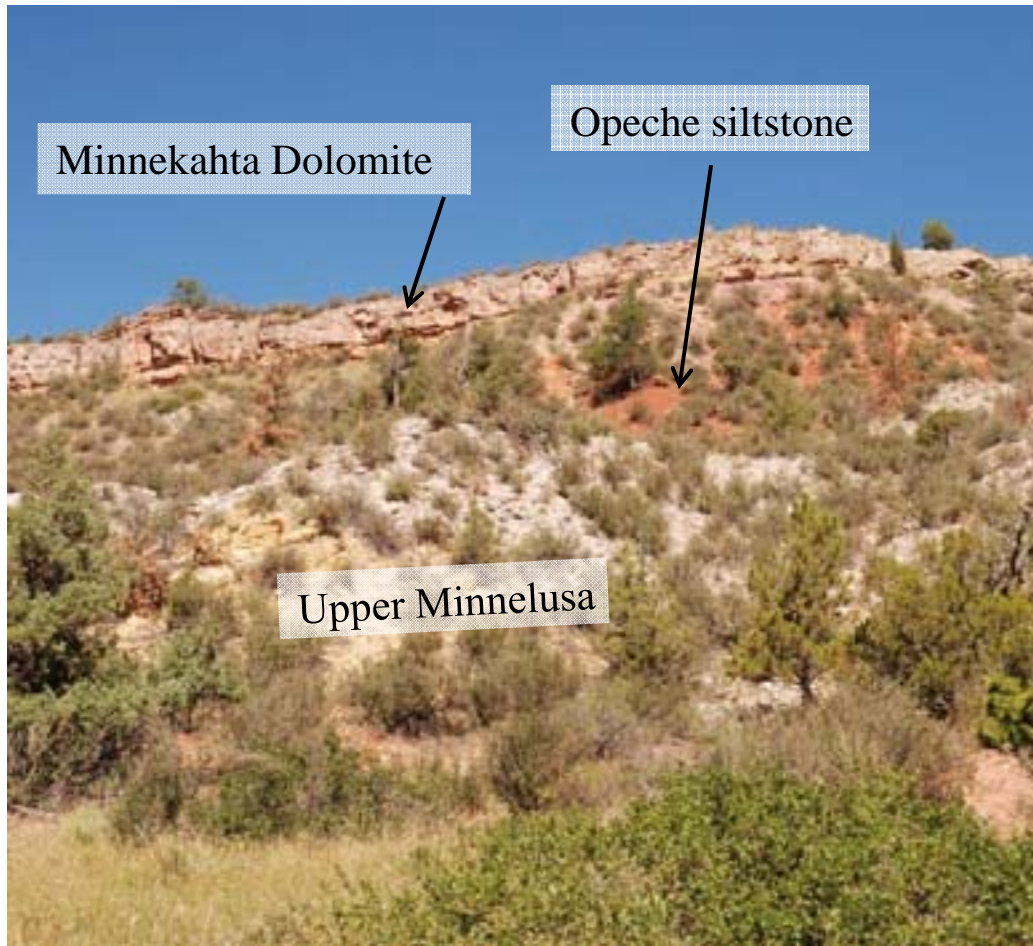


Sabkha sands in Middle Minnelusa

5. Redbird Canyon: *Field localities*

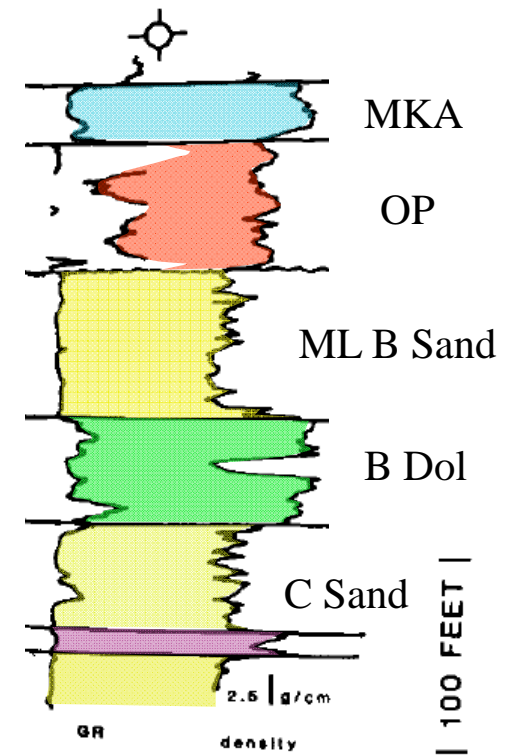


5. Redbird Canyon: Road to Redbird Canyon 1, Upper Minnelusa, Opeche and Minnekahta



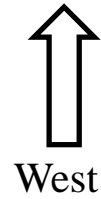
Upper Minnelusa sands (white), Opeche and Minnekahta on skyline. On road to Redbird Canyon.

Tenneco Oak Nelson Canyon
T53N R65W NE SW 10



GR-Sonic logs from a Minnelusa well in the play area opposite the outcrops. After Fryberger, 1984

5. Redbird Canyon Area: Intersection of Boles Canyon Road (FDR 117) and Roby Canyon Road:
Upper Minnelusa, Opeche and Minnekahta



5. Redbird Canyon Area: Intersection of Boles Canyon Road (FDR 117) and Roby Canyon Road: *Upper Minnelusa, Opeche and Minnekahta*

Upper Minnelusa sedimentology



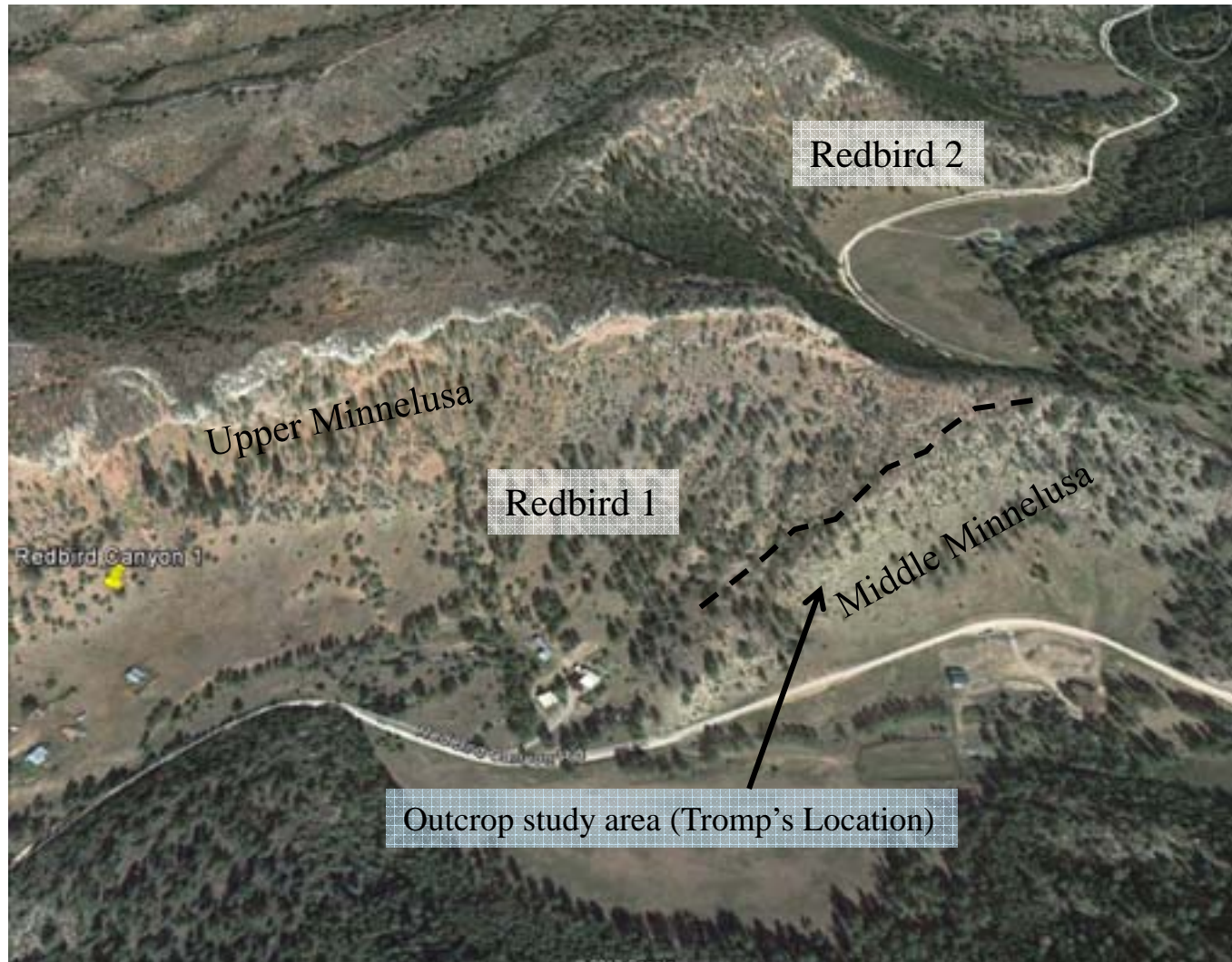
Cliff of Upper Minnelusa on Boles Canyon Road. Irregular and broken up aspect is due to dissolution of evaporites in underlying Minnelusa.

The Upper Minnelusa in this area has most of the features typical of eolian deposition, however the rocks have been broken up in part by faults and collapse associated with dissolution of evaporites. It is still possible to identify original genetic units in outcrop. Open fractures such as those seen here in outcrop will cause increased production rates, although they may also create bypassing and poor overall sweep depending upon specific field parameters and production techniques.



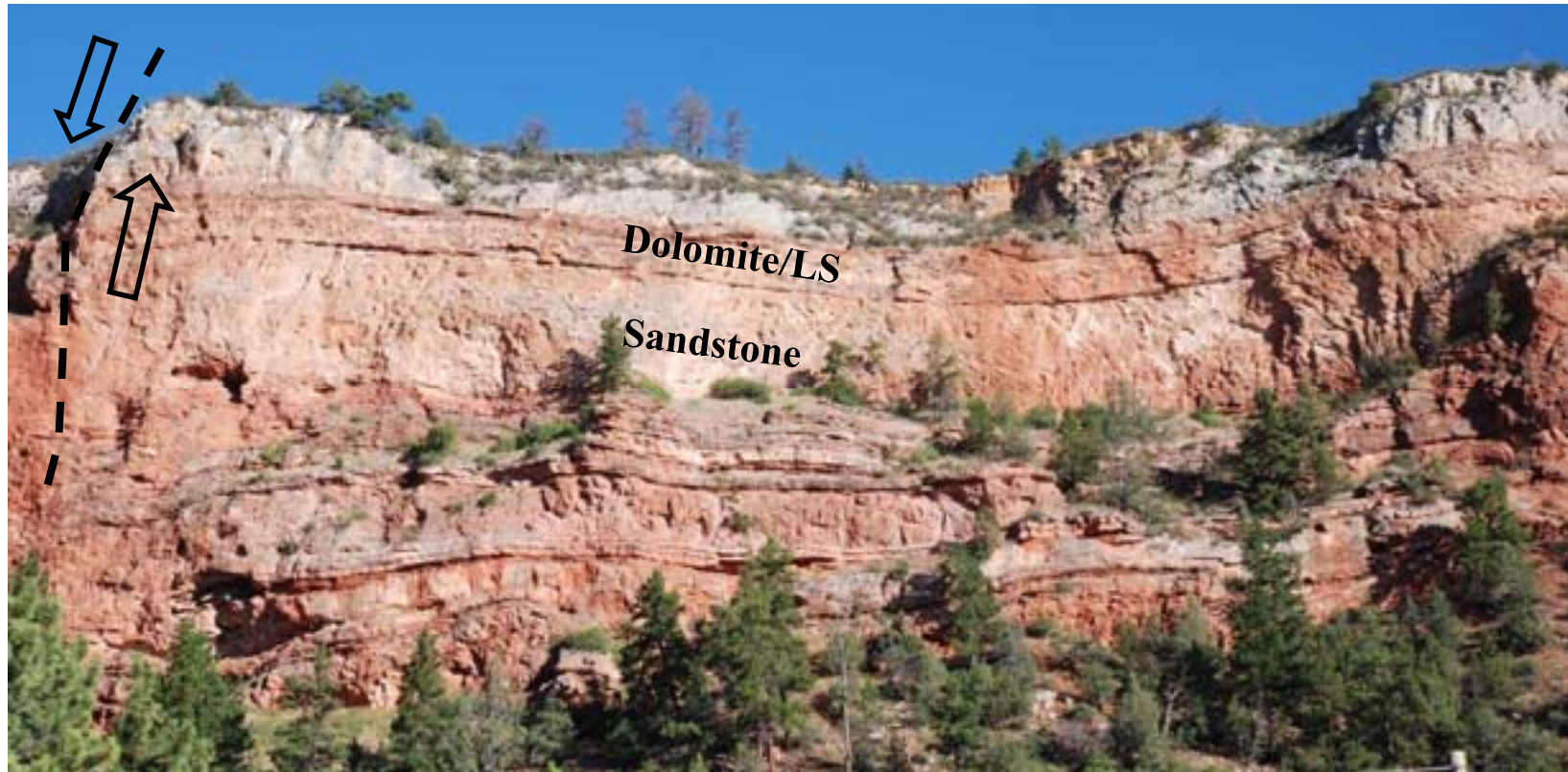
Eolian cross lamination, inverse graded and fractured

5. Redbird Canyon: *Outcrop localities 1 and 2 (views) and outcrop study area (After Tromp 1981, 1984)*



5. Redbird Canyon (1): *Upper Minnelusa sands and dolomites*

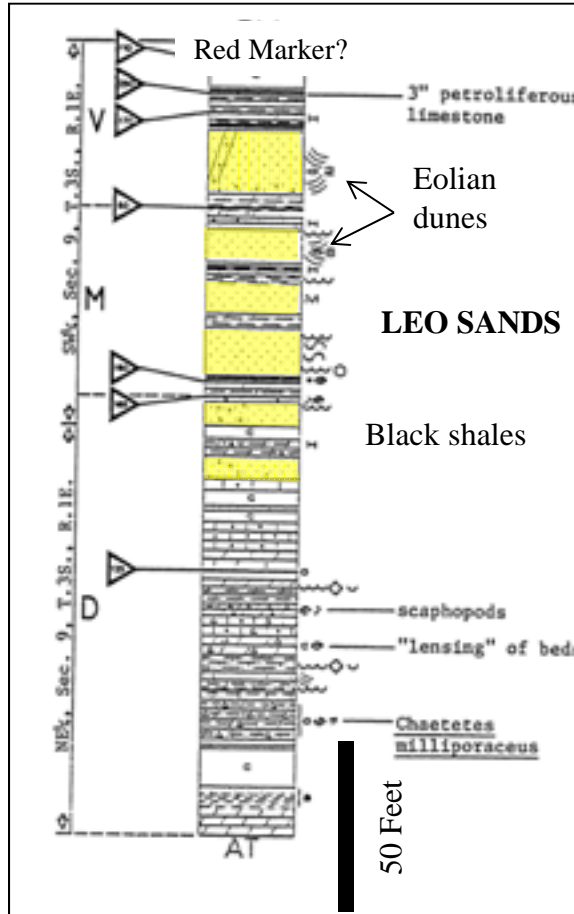
Edge of solution-collapse structure



Alternating recessed eolian sandstones and resistive dolomites of the Upper Minnelusa Formation, Redbird Canyon, South Dakota. Displacement on the left is the edge of a graben formed by dissolution of evaporites, followed by solution-collapse.

5. Redbird Canyon (1) (*Tromp's locality*) *Middle Minnelusa near-shore marine carbonates and eolian dunes*

The Middle Minnelusa at this outcrop represents a “drying upward” sequence, as dunes become more and more important in the outcrop towards the top. The Upper Minnelusa Formation above represents the culmination of this process, with extensive evaporites replacing marine dolomites and limestones, and influx of dune fields over the region.



Measured Section of the Middle and Lower Minnelusa Formation, Redbird Canyon, South Dakota. After Tromp, 1981, 1984



Outcrop section in **Middle Minnelusa**. Shaly Middle Minnelusa transitions upward to eolian dune and sabkha sediments weathering as resistive units near the top of the slope.

5. Redbird Canyon (1) Middle Minnelusa: *Sedimentology of aeolian sabkha and dune sands*

Ancient Minnelusa eolian sabkha



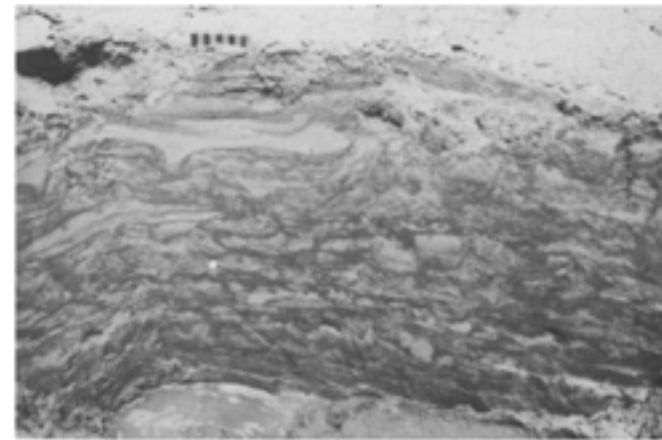
Eolian sabkha deposits, consisting of irregular strata formed by salt ridges with some interbedded eolian laminations.

Fryberger, Jones and Johnson, 2014

Modern Saudi Arabian eolian sabkha



Salt ridge and shallow layer of freshly deposited sand (white material) near trap 11. Pencil gives scale.

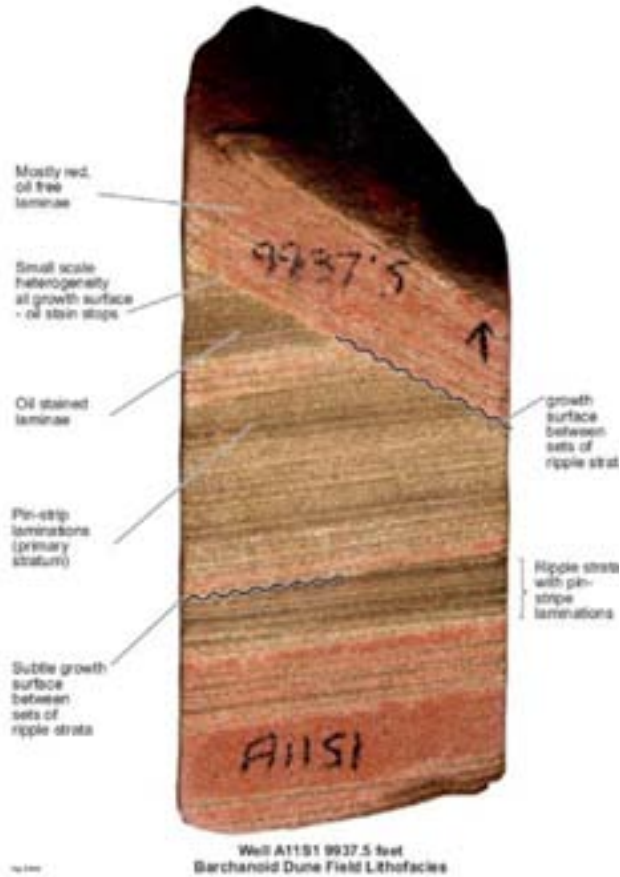


Trench in sabkha at site 7, showing irregular layers resulting from slow upward growth of sabkha by episodic deposition of sand, followed by salt ridge formation. Water table is at base of trench. Bars on scale at upper left are 1 cm in width.

Modern salt ridge structures formed on a sabkha along the Arabian Gulf. After Fryberger, et al, 1984

5. Redbird Canyon (1) *Middle Minnelusa, Permeability of aeolian dune sands*

Much of the critical flow effects of eolian cross bedding and cross strata are due to strong differences in porosity and permeability between individual laminations, as illustrated in the two figures below. The isolation of permeable laminae by tight laminae may drastically reduce sweep efficiency in rocks that, on standard logs and core plugs, appear quite permeable. These microfabrics also, potentially, create anisotropic sweep tendencies in the rocks.



Core from eolian strata in Auk Field, Permian Rotliegend sandstone, UK. North Sea. Brown laminae are oil stained, red laminae have no oil. After Trewin, Fryberger and Kreutz, 2003

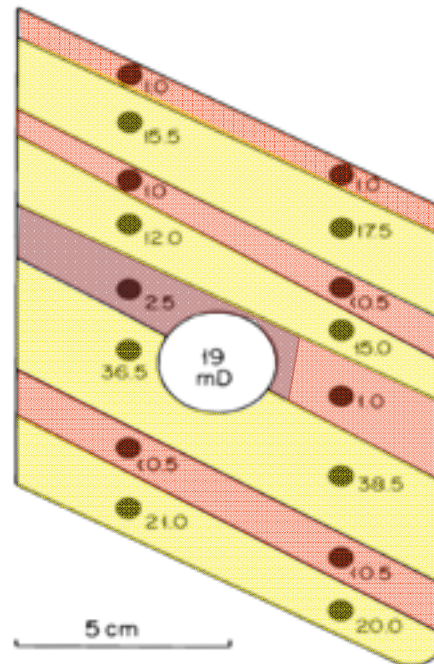


FIG. 17.—Aeolian core slab with a dense grid of mini-permeameter permeability readings. Aeolian crossbed set boundaries are indicated.

Laminar –scale variability of permeability, measured with a minipermeameter. After Weber, 1987



Stacked sets of eolian avalanche and Ripple strata, Middle Minnelusa. Some erosional bounding surfaces highlighted with black lines.

5. Redbird Canyon (1) *Upper Minnelusa in core*

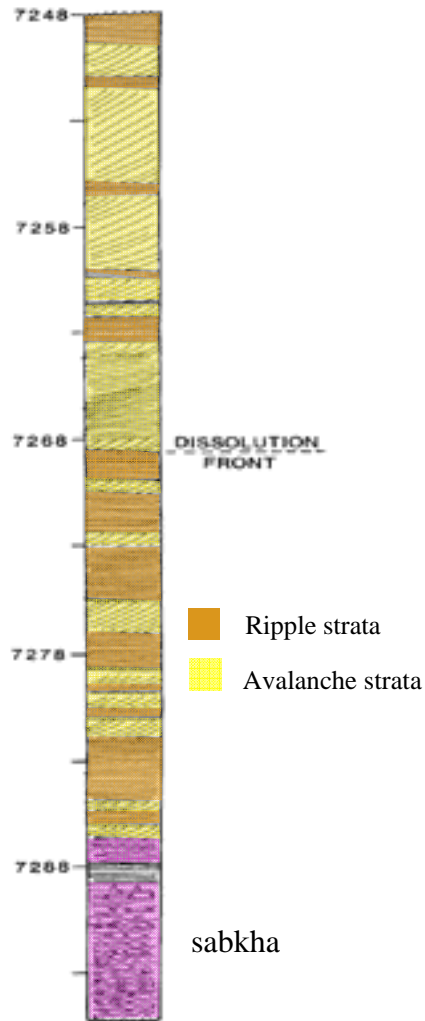


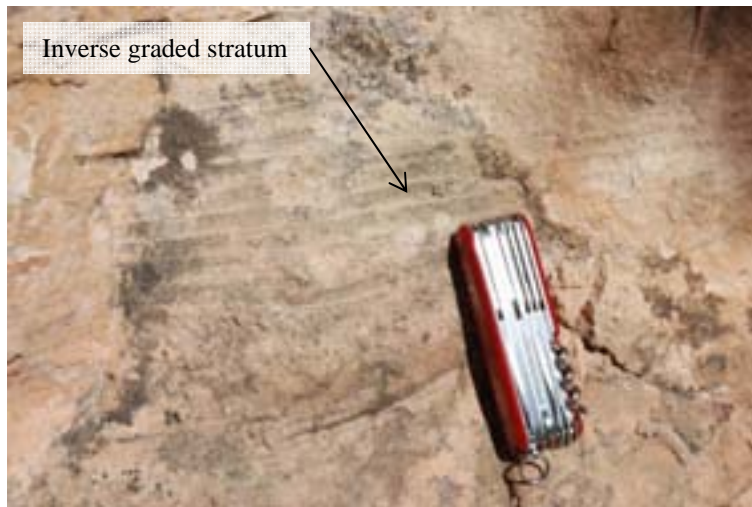
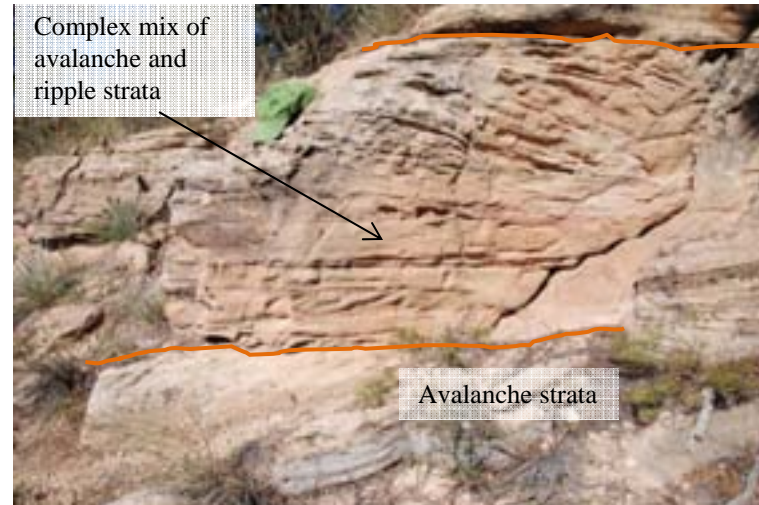
FIGURE 10. SEDIMENTOLOGIC LOG FOR CORE 6, SANDSTONE OF THE PERMIAN UPPER PART OF THE MINNELUSA FORMATION, DAVIS OIL CO., #1 SCHWINN-FEDERAL, SEC. 9, T. 52 N., R. 68 W., WEST MELLOTT FIELD, CAMPBELL COUNTY, WYOMING.

Core from the Upper Minnelusa at West Mellott Field, showing dune, interdune and sabkha deposits

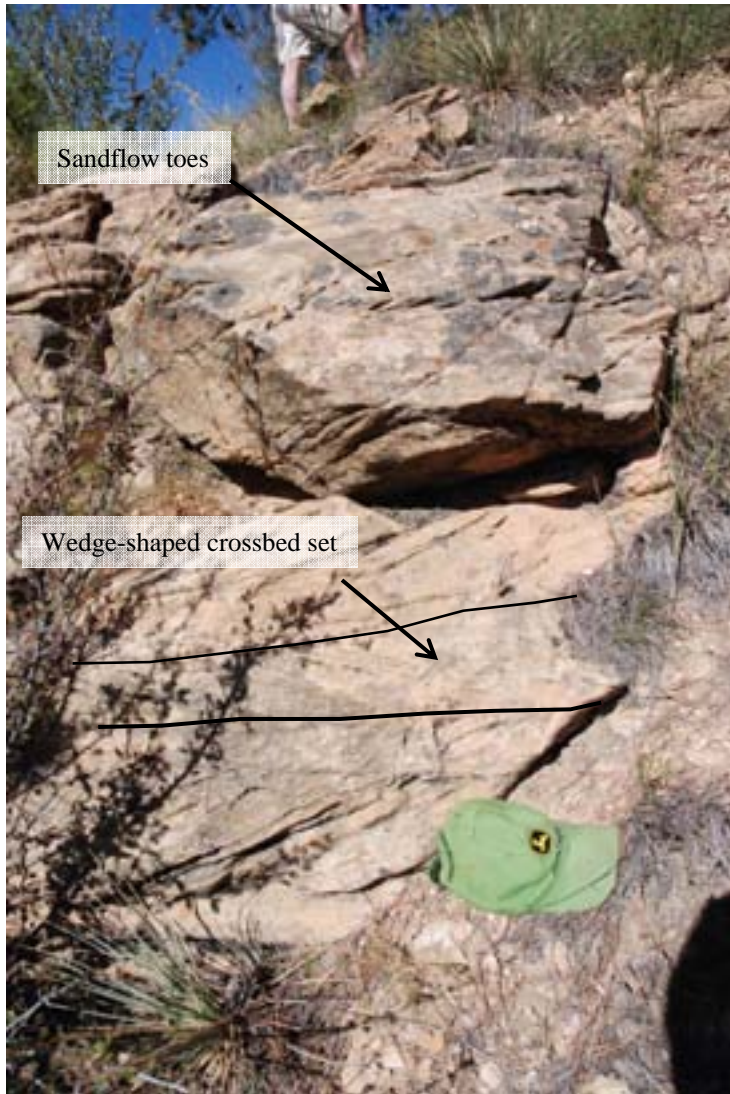


Core from the Upper Minnelusa at the Pan Am 68 Unit Well, showing oil-stained eolian cross lamination. Despite the even stain, differences in permeability among individual laminae may complicate sweep of hydrocarbons to the producing wellbore.

5. Redbird Canyon (1) *Middle Minnelusa aeolian dune sands*



5. Redbird Canyon (1) *Middle Minnelusa aeolian dune sands*

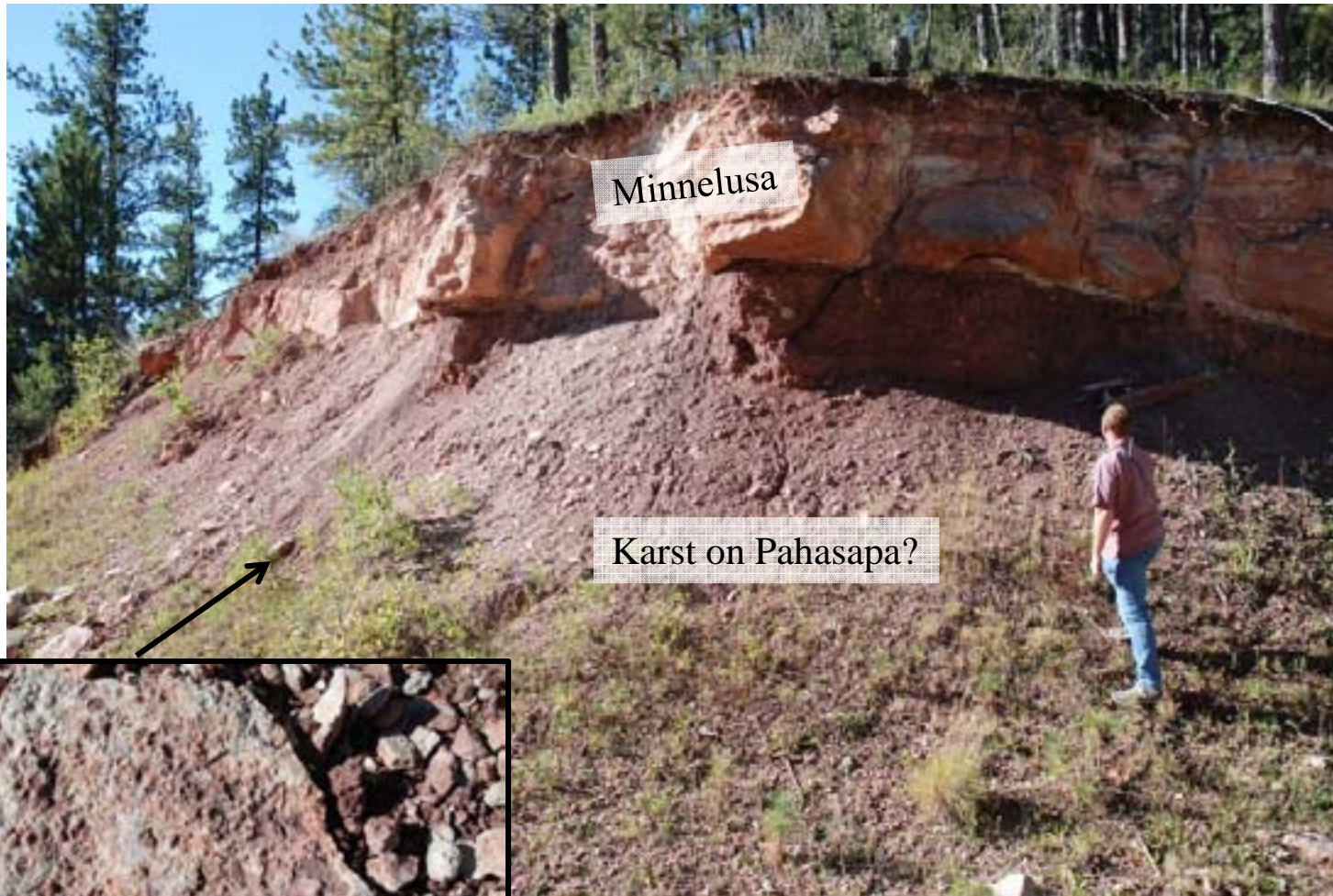


Wedge-shaped lamination sets in eolian Minnelusa



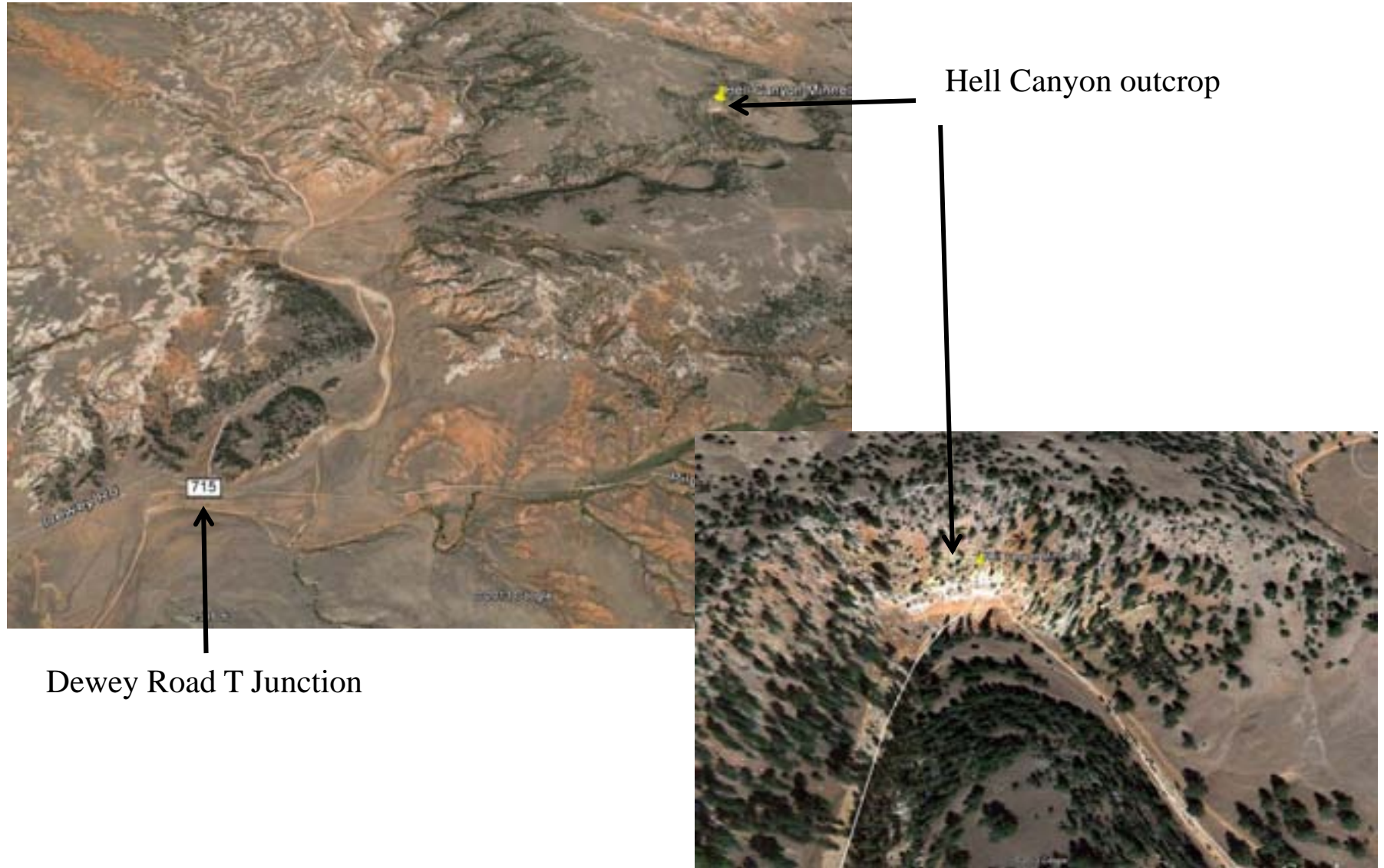
Stack of inverse-graded cross strata, multiple cross bed sets

5. Redbird Canyon: *Minnelusa* contact with *Pahasapa* (Karst?)



Siltstone pebbles in limestone.

6. Hell Canyon, South Dakota: *Upper Minnelusa eolian and evaporite deposits*

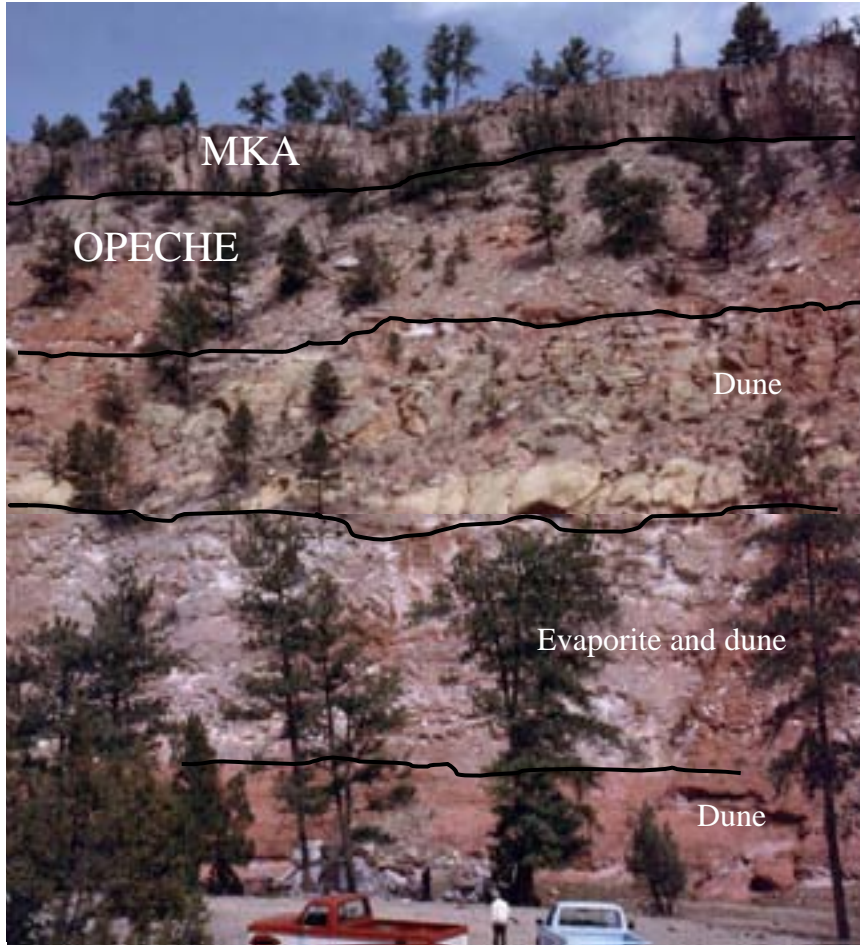


Hell Canyon outcrop

Dewey Road T Junction

6. Hell Canyon, South Dakota: *Upper Minnelusa eolian and evaporite deposits*

This is an excellent outcrop to view basic Minnelusa eolian facies interbedded with evaporites.



Hell Canyon Upper Minnelusa outcrop



Eolian avalanche strata in the redbeds at base of the cliff



Contact of eolian sand above and evaporites below



Pin stripe laminations produced by eolian ripples

6. Hell Canyon, South Dakota: *Upper Minnelusa eolian and evaporite deposits*



Eolian sabkha bedding mixed with dry wind ripple laminations

Eolian strata, slightly irregular.. These strata tend to be the best reservoir in eolian rocks



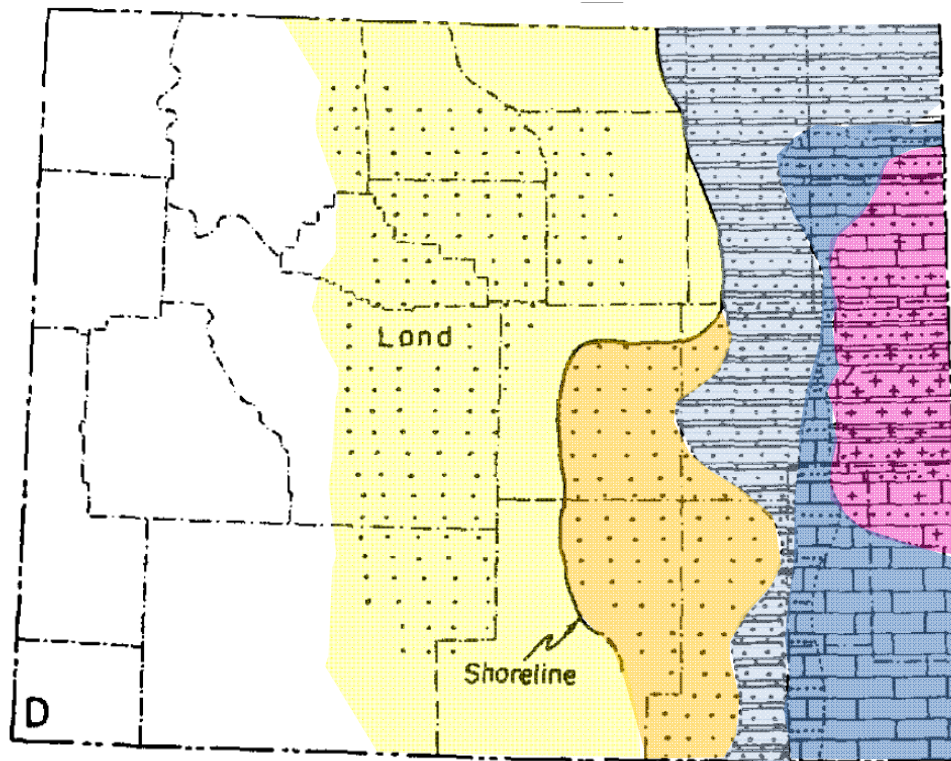
Eolian avalanche strata showing individual sand flows separated by pin-stripes



Avalanche strata and pin stripes

7. Minnelusa Regional Geology: *Permian Facies Map*

This 1954 lithofacies map by Agatston is interesting because it shows the evaporites in the Black Hills, and the carbonates of the Lusk Embayment to the south. Generalized loss of carbonates into the dune fields of Central and Western Wyoming is accurate for Lower Permian rocks, in general. Compare with Fryberger figure on page 41 showing the Lusk Embayment, based on drilling in the Minnelusa play through 1984..



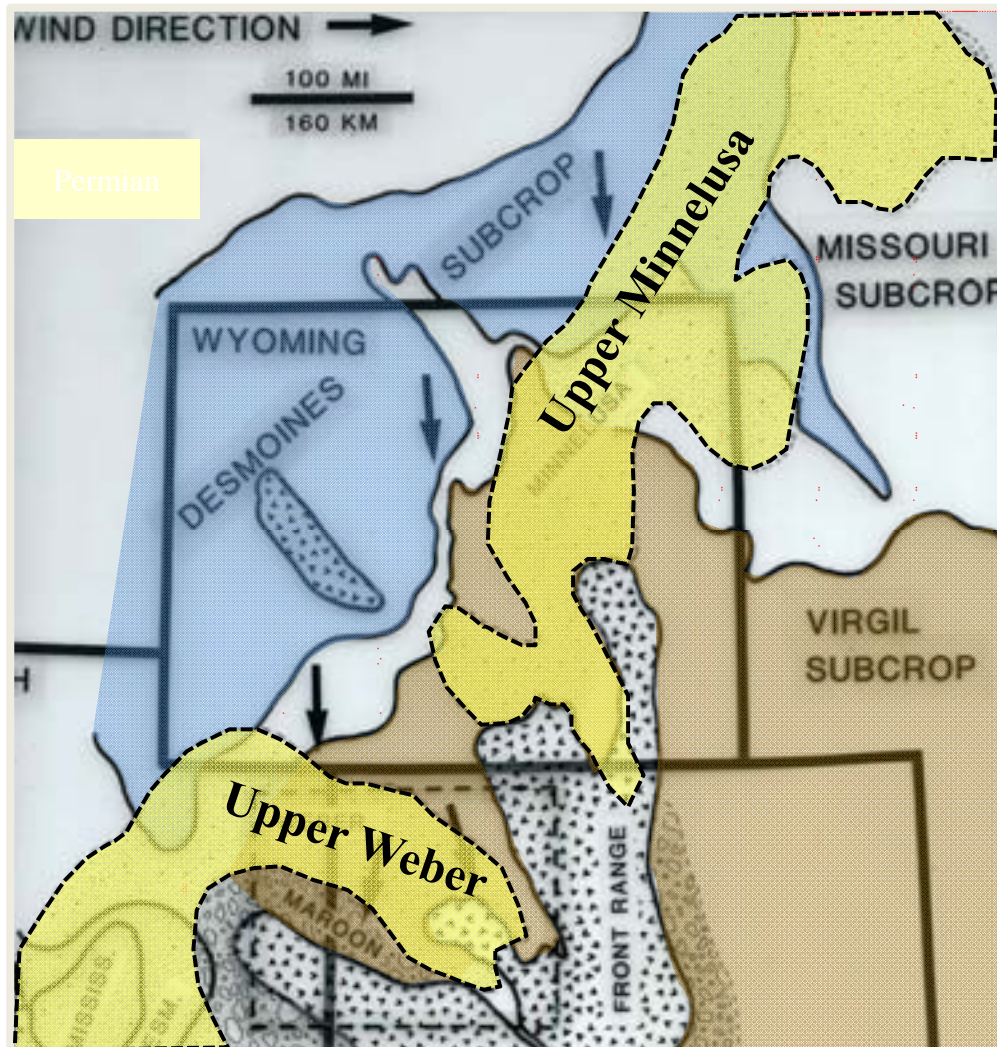
Lithofacies map of Eastern Wyoming during Lower Permian.
After Agatston, 1954

Below: Typical lithological distinctions between Pennsylvanian and Permian Rocks, SE Wyoming.
After McKee et al, 1967

The Permian parts of the formations differ from the Pennsylvanian as follows:

1. Permian detrital strata are generally orange red to brownish red, whereas the Pennsylvanian beds are gray above and purplish red below.
2. Evaporites in thick beds are common in Permian strata, but they are thin bedded or sparse to absent in the Pennsylvanian. Evaporites have mostly been leached from surface exposures, but their former positions are indicated by sandstone and limestone breccia, which are common in the upper parts of the Minnelusa and Hartville Formations (Bowles and Braddock, 1960; Condra and others, 1940).
3. Radioactive black shaly mudstone occurs at several horizons in the Pennsylvanian but is unknown in the Permian.
4. Sandstone units within the Permian part of each formation commonly include scattered larger quartz grains, whereas sandstone in the Pennsylvanian part is of nearly uniform grain size.
5. Limestone is common in Pennsylvanian strata but rare in Permian strata, although dolomite is common in both.
6. The Permian parts of each formation and the lower parts of the Pennsylvanian are generally uniform in thickness and lithology, and their composition and position are predictable from place to place. The Upper Pennsylvanian strata differ widely in thickness because of an unconformity at their top.

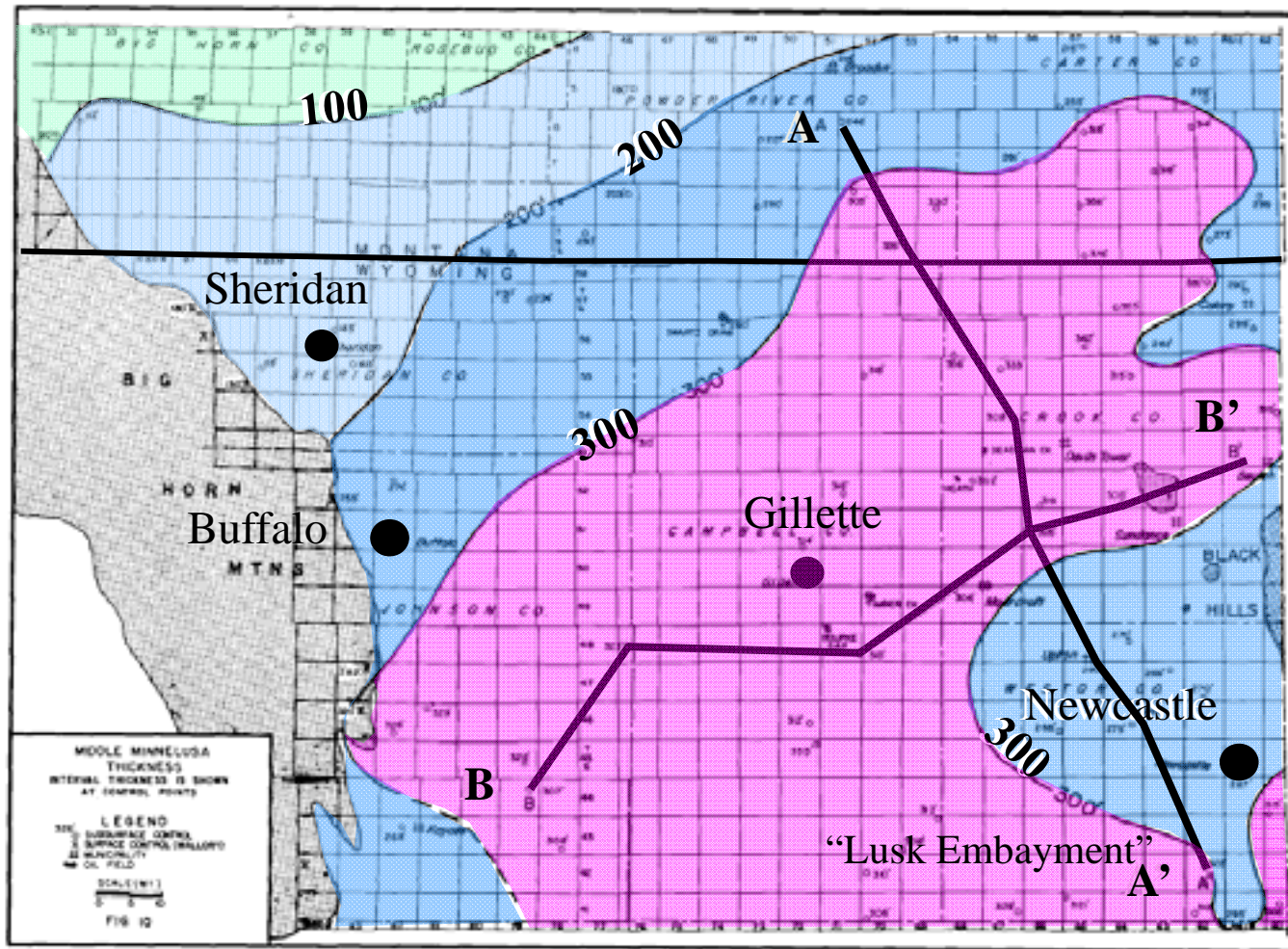
7. Minnelusa Regional Geology: *Minnelusa-Tensleep* age relationships



The slide on the left follows the classic 1972 map by Rascoe and Baars showing the Distribution of Permian Upper Minnelusa (yellow) overlain on the underlying sandstones of Pennsylvanian age. These maps define an oil and gas play fairway extending from Montana through Utah.

(after Rascoe and Baars in RMAG Atlas, 1972)

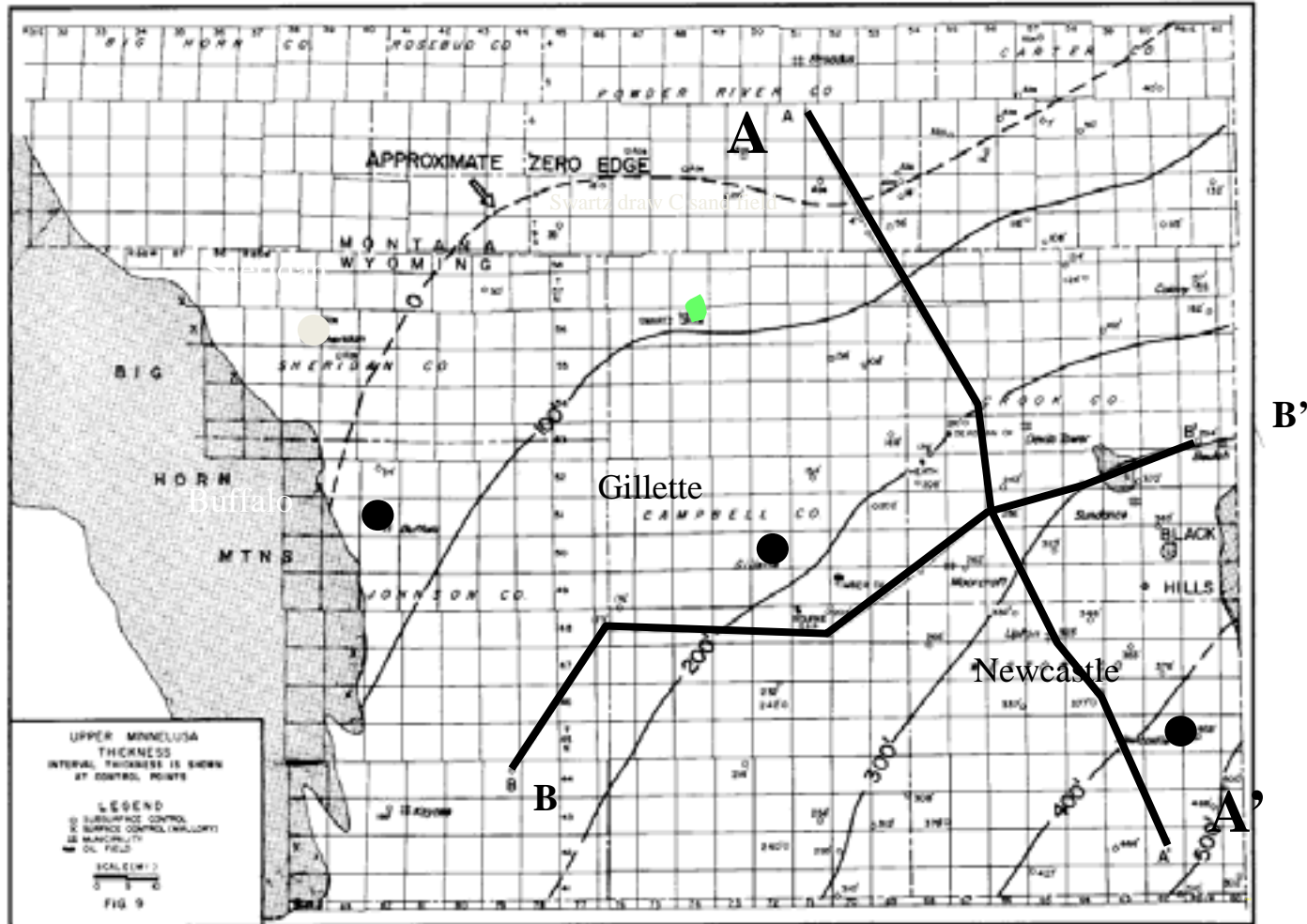
7. Minnelusa Regional Geology : *Middle Minnelusa isopach*



Middle Minnelusa Thickness (ft.) Desmoines, Missouri, Virgil
 . After Trotter, 1984

Cross sections are shown on
 page 35.

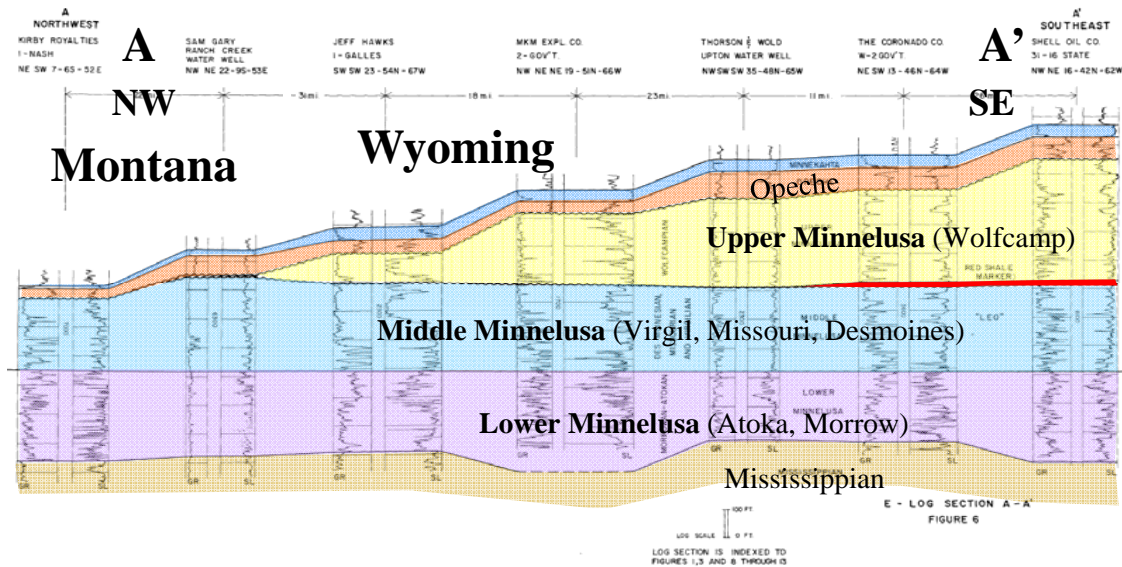
7. Minnelusa Regional Geology : *Upper Minnelusa Isopach*



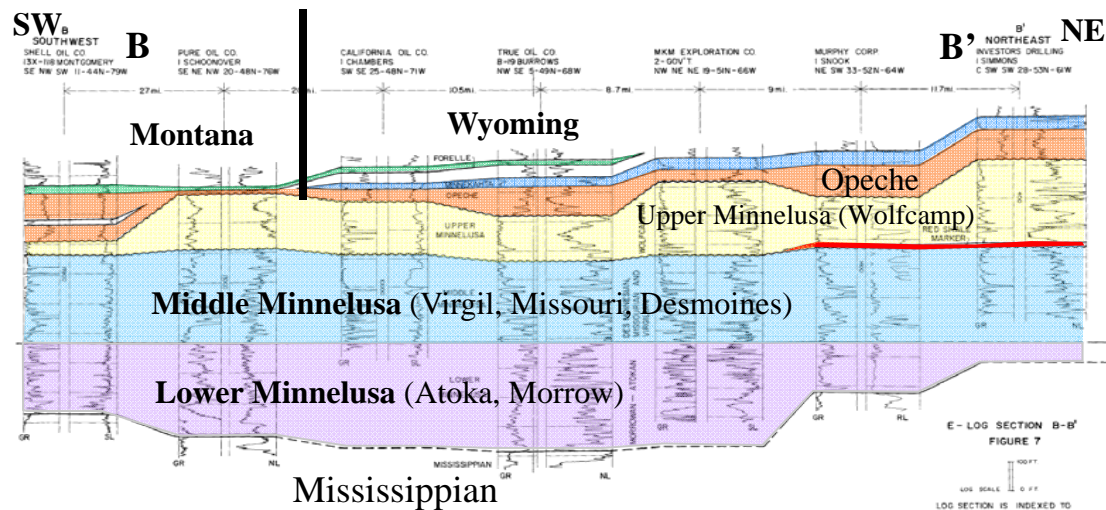
Upper Minnelusa Thickness (ft.). After Trotter, 1984

Cross sections are shown on page 35.

7. Minnelusa Regional Geology: Regional Cross sections



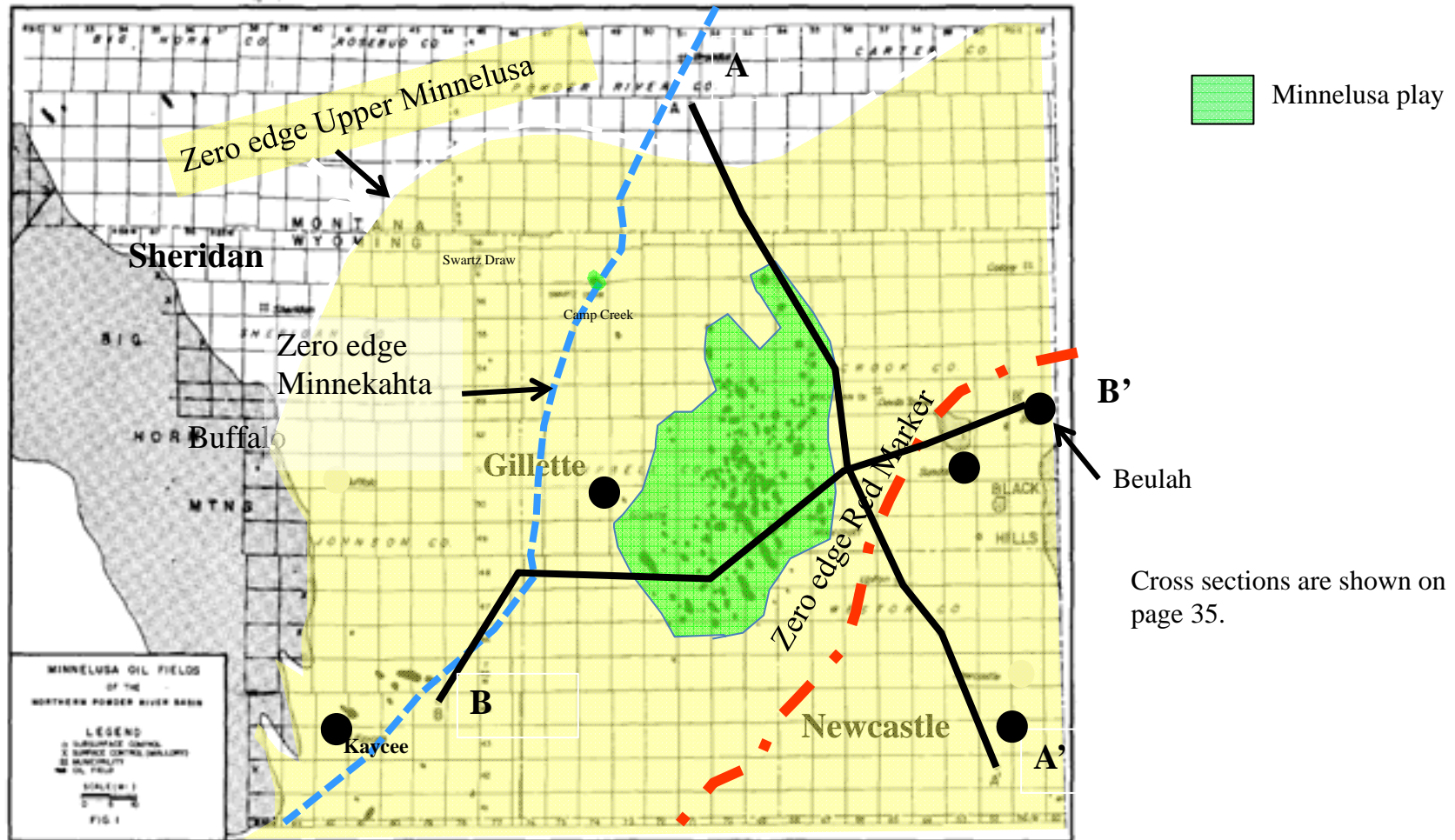
Minnelusa Cross Section A-A'. After Trotter, 1984



SW to NE Minnelusa Cross Section B-B'. After Trotter, 1984)

The routes of these cross sections is shown on pages 33 and 34

7. Minnelusa Regional Geology: *Minnelusa Play Fairway*



Minnelusa Oil Fields: Northern Powder River Basin after Trotter, 1984

7. Minnelusa Regional Geology: *Minnelusa production by zone*

Oldest

Youngest



C Sand



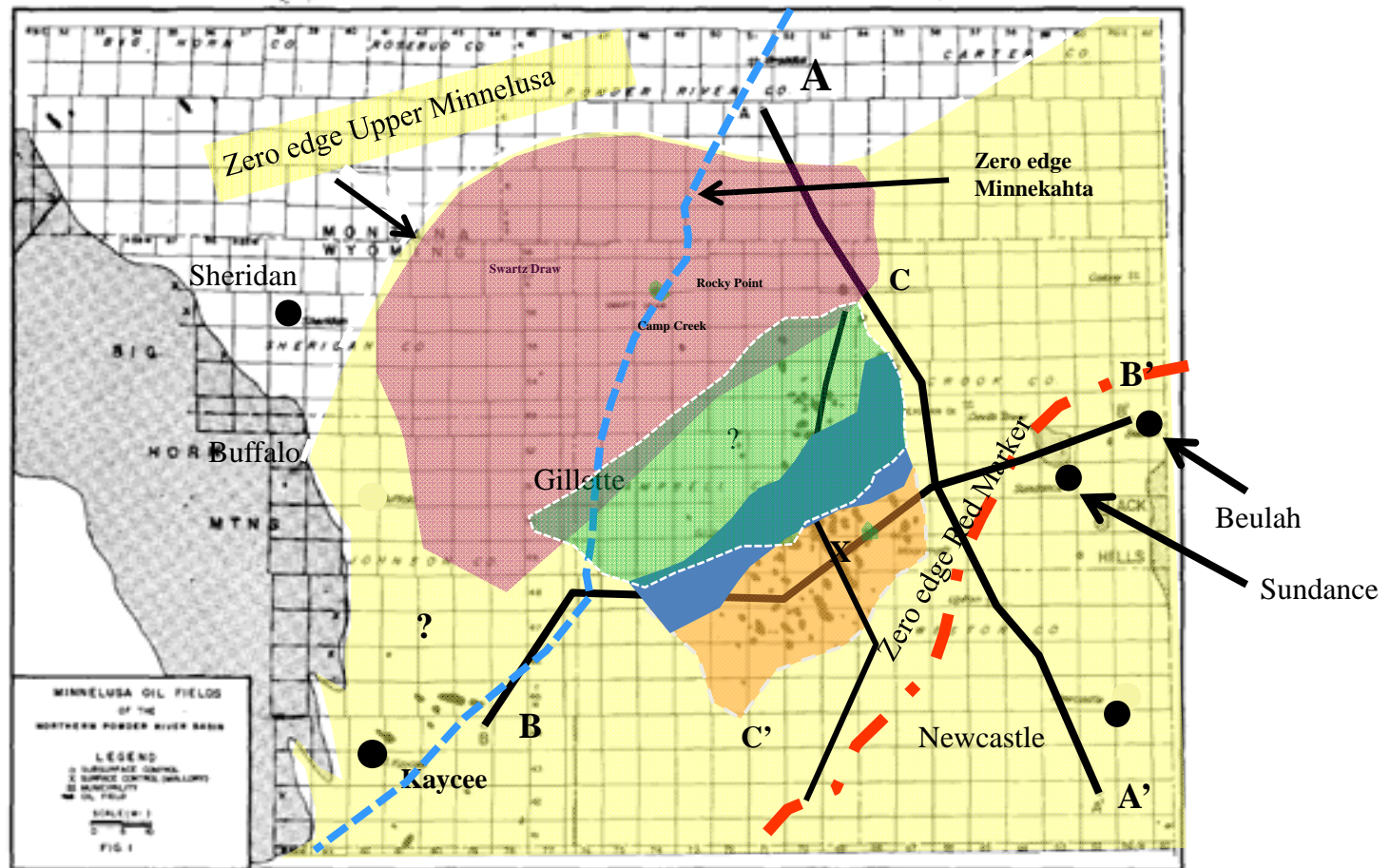
B Sand



Upper B Sand



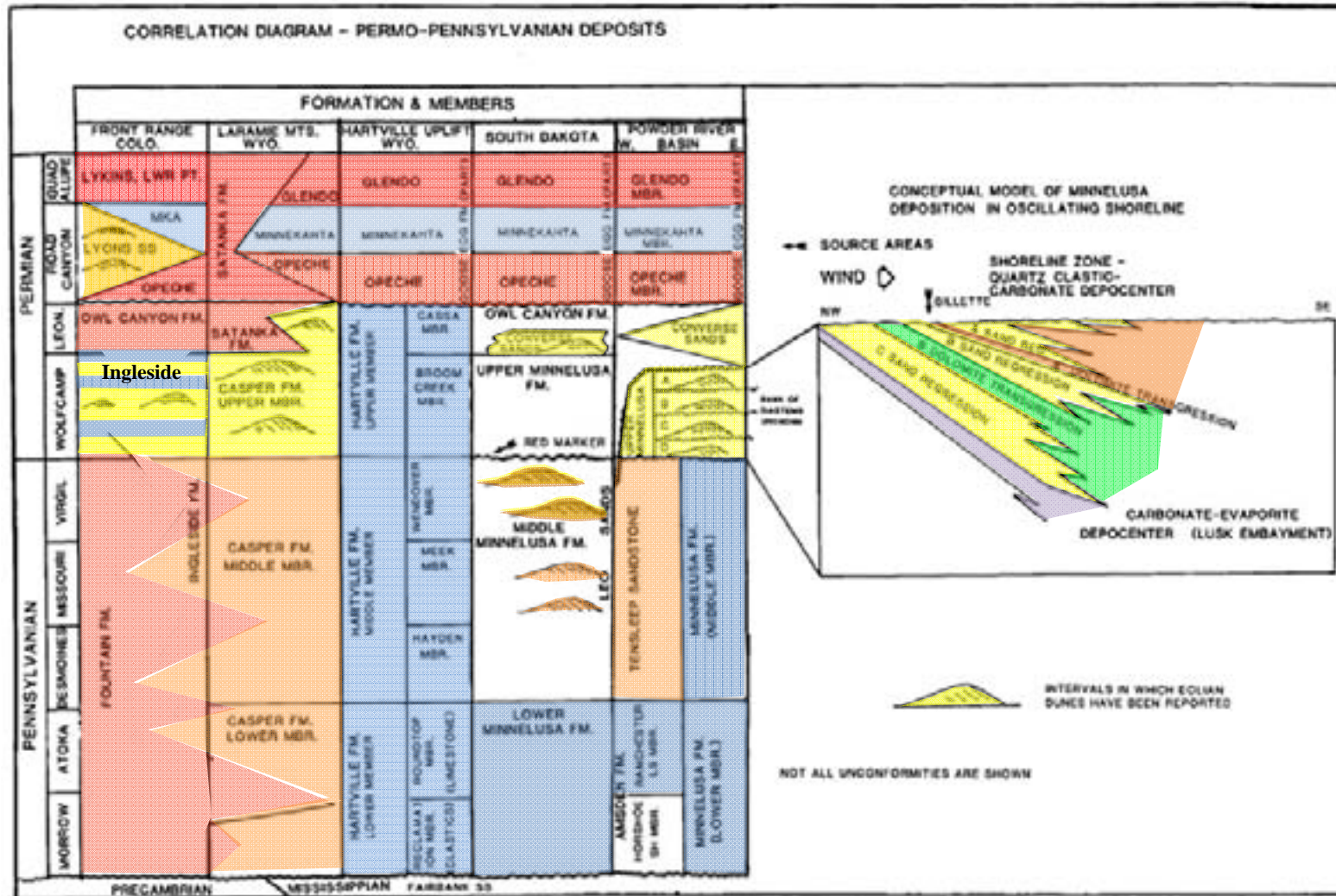
A Sand



Minnelusa Production fairways by Stratigraphic unit (sands) After Trotter, 1984

7. Minnelusa Regional Geology: Correlation diagram Permo-Penn

This correlation diagram is focused on the distribution of various sands in the Permo-Pennsylvanian rocks that are considered to be eolian by most workers. Most have oil or gas production somewhere in the Rockies.

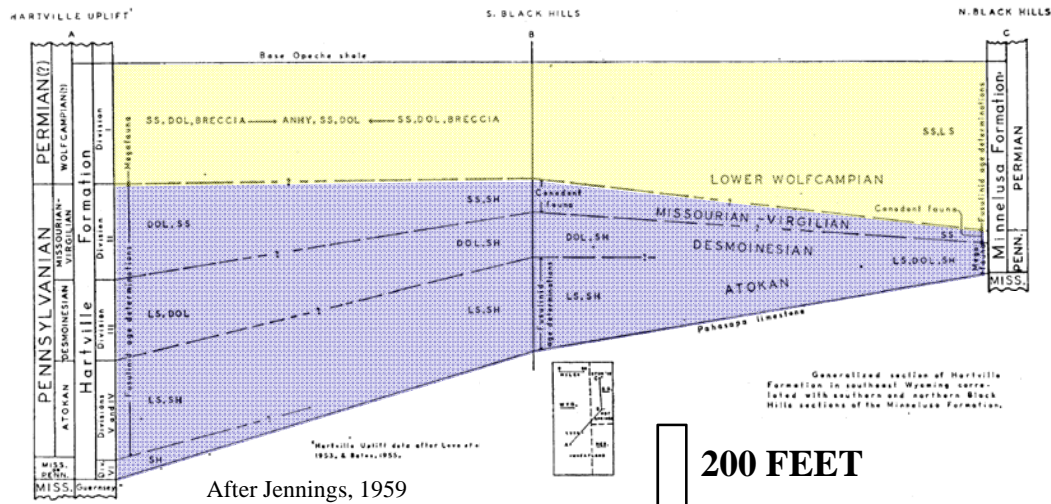


After Fryberger, 1984

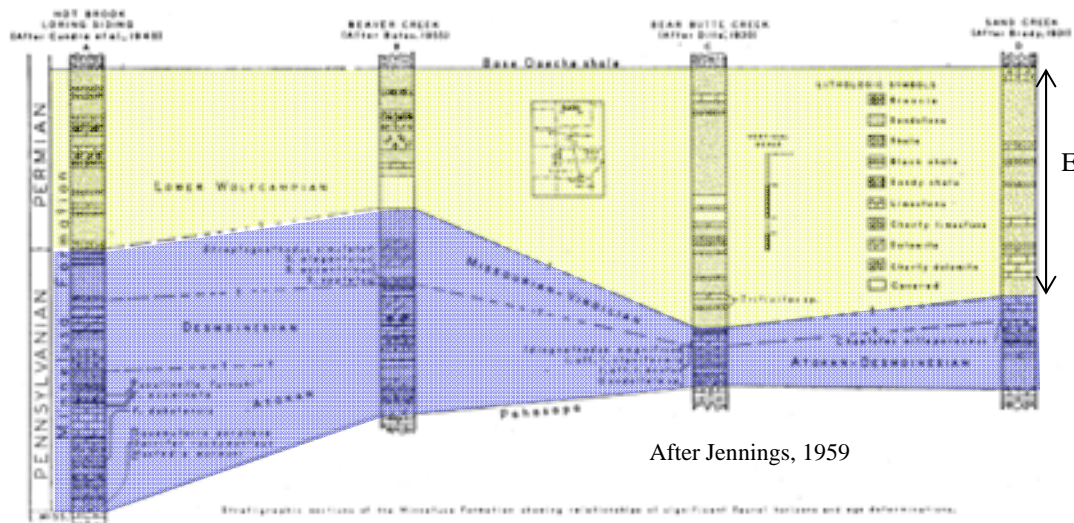
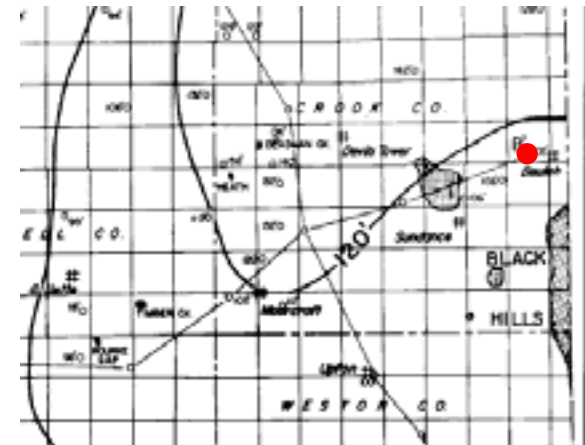
Fryberger, Jones and Johnson, 2014

38

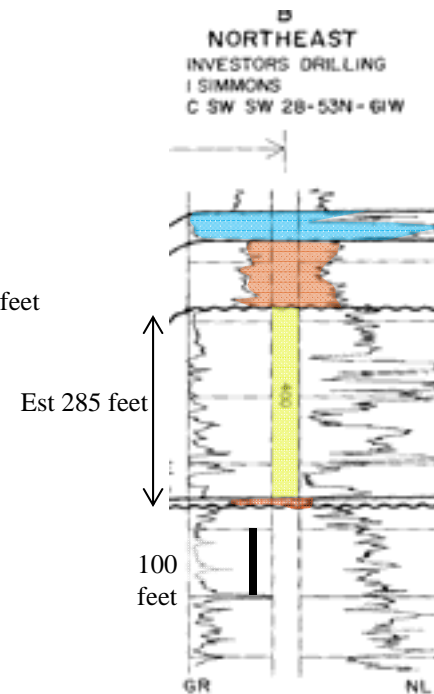
7. Minnelusa Regional Geology: Stratigraphy of Minnelusa Formation in the Black Hills



TEXT-FIG. 2—Generalized section of Hartville Formation in southeast Wyoming correlated with southern and northern Black Hills sections of the Minnelusa Formation.



TEXT-FIG. 1—Stratigraphic sections of the Minnelusa Formation showing relationships of significant faunal horizons and age determinations.



7. Minnelusa Regional Geology: *Minnelusa/Tensleep sedimentation styles*



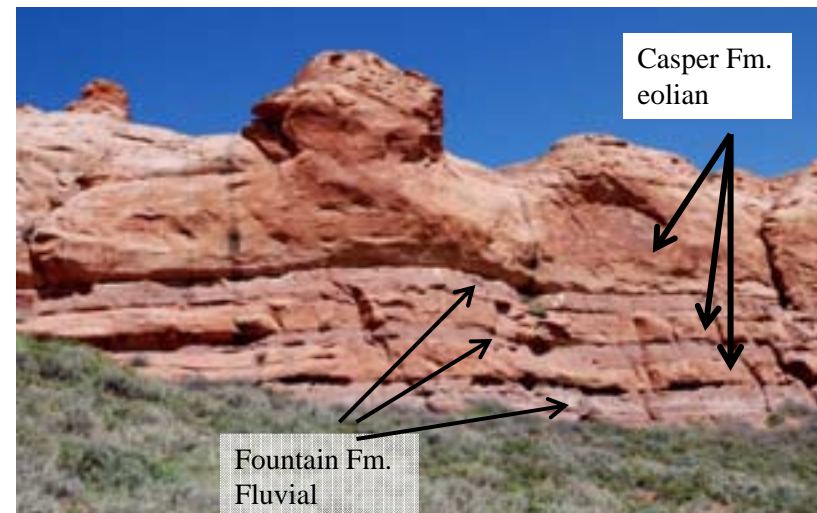
Middle Minnelusa at Guernsey Reservoir, Wyoming: marine limestones interbedded with shoreline and eolian sandstones of the Lusk Embayment.



Ingleside Formation at Owl Canyon, near Livermore, Colorado: Lower Permian marine Carbonates interbedded with eolian dunes and sabkhas. View to north.



Tensleep Formation at Flat Tops near Medicine Bow, Wyoming: Crossbedded eolian dunes impregnated with oil, and barren flat bedded eolian sabkha deposits

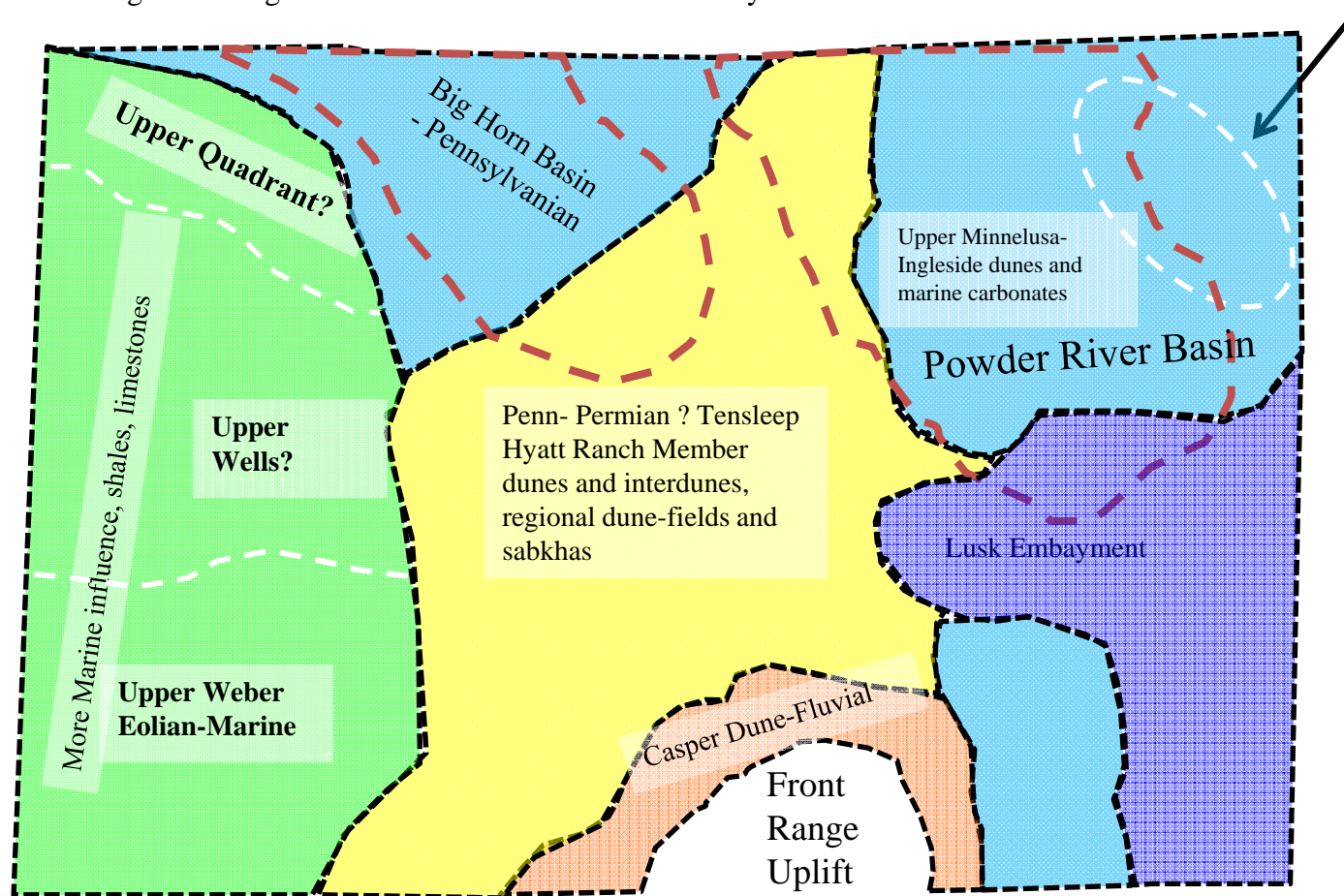


Casper Formation at Sand Creek near Laramie, Wyoming: Permo-Pennsylvanian Crossbedded eolian dunes interbedded with Fountain Formation fluvial sands

7. Minnelusa Regional Geology: *Lithological styles in the Permo-Pennsylvanian rocks of Wyoming*

This diagram is presented for discussion. It shows realms of sedimentation in the Permo-Pennsylvanian rocks in order to illustrate different lithological styles – regardless of age. The edge of known Permian rocks is shown by the dashed line.

Field trip area in Black Hills



Realms of Tensleep sedimentation: facies style

Different colors represent unique styles of sedimentation. These different styles of sedimentation result in different reservoir flow properties and flow units.

8. Modern and Ancient analogues: *Basic Dune Types*

Modern Analogues: Eolian dune type and formative wind regime

Dune types depend upon wind direction



Barchanoid – 1 wind direction



Linear – 2 main wind Directions



Star – 3 main wind Directions

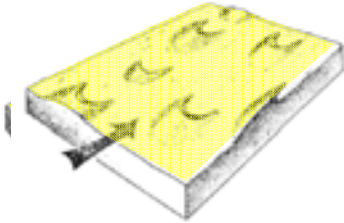
After Fryberger, 1979

8. Modern and Ancient analogues: *Basic Dune Types with barchanoid subtypes*

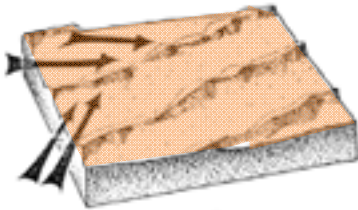
Dune type sets the basic arrangement of cross-strata within an eolian genetic units that ultimately becomes part of an eolian reservoir.

Dune types and sub-types

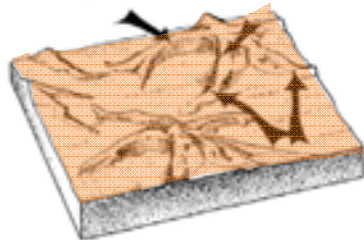
Basic Dune types



Barchan dunes. Arrow shows main wind direction

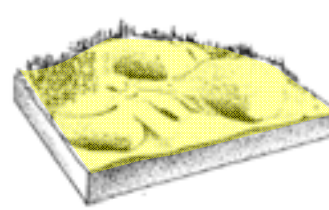


Linear dunes. Arrows show two main wind directions

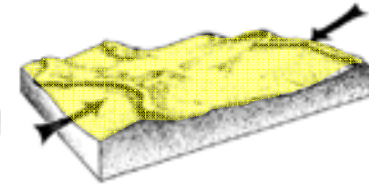


Star dunes. Arrows show three main wind directions

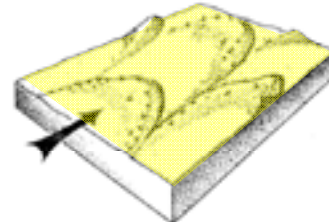
Barchanoid dune sub-types



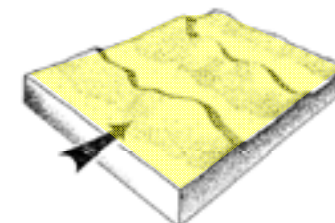
Blowout



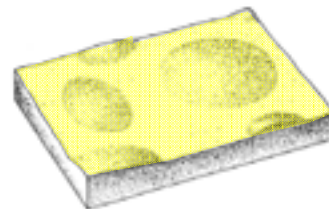
Reversing



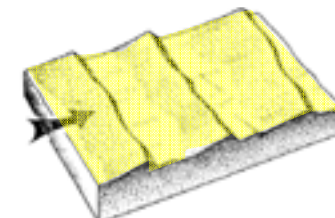
Parabolic



Barchanoid ridge



Dome



Transverse ridge

Dune varieties produced in unidirectional wind regimes, after Fryberger, 1979.

After Fryberger, Krystinik and Schenk, 1991

8. Modern and Ancient analogues: *Basic eolian cross bedding and facies*

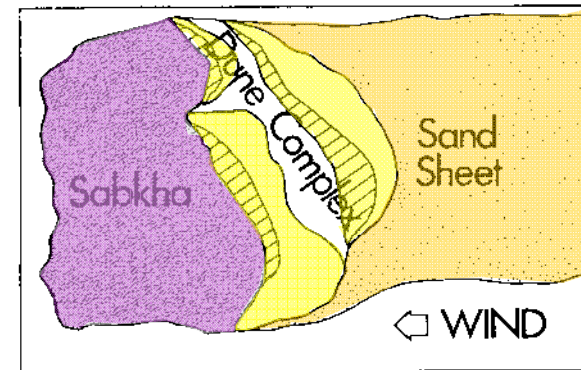
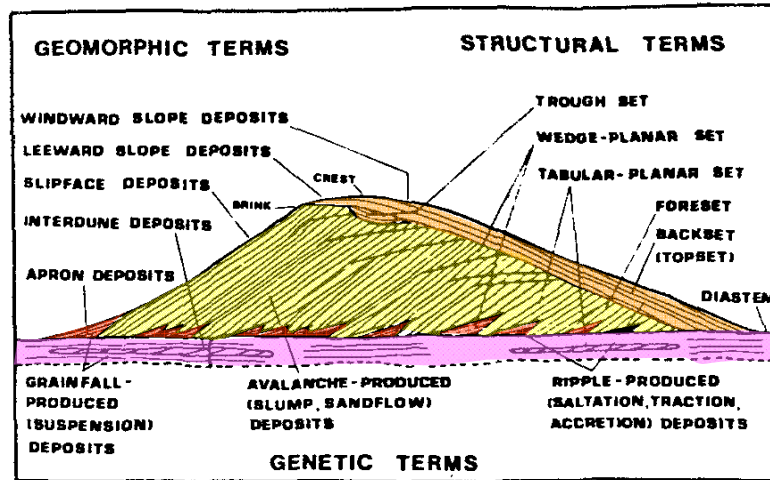


FIGURE 5 - THE FOUR EOLIAN FACIES. INTERDUNES ARE BETWEEN DUNES IN THE "DUNE COMPLEX."

TABLE I SEDIMENTARY FEATURES OF PRIMARY EOLIAN STRATA

STRATA TYPE	FEATURE
GRAINFALL	<ul style="list-style-type: none"> RAPID THICKNESS CHANGES Laterally WITHIN LAYERS IRREGULAR THICKNESS FROM LAYER TO LAYER NORMAL OR INVERSE GRADING INDISTINCT LAMINATION STYLE
AVALANCHE	<ul style="list-style-type: none"> 1-4 CM THICKNESS SANDFLOW TOES, W/COARSE GRAINS INVERSE GRADING FADEOUT LAMINAE FLAME STRUCTURES BREAK APARTS (DAMP SAND) LOBATE FORM IN BEDDING PLANE VIEW PIN-STRIPE LAMINATION ALONG BASE OF FLOW GENTLE WAVINESS OF STRATUM
RIPPLE	<ul style="list-style-type: none"> EVEN, VERY DISTINCT LAMINATIONS 1-4 MM THICK RIPPLE FORESETS HIGH INDEX OF RIPPLES (HIGH WIDTH-HOT RATIO) (ABOUT 10-20) INVERSE GRADING PIN-STRIPE LAMINATION STYLE RELATIVE CONTINUITY VIS-A-VIS GRAINFALL.
ADHESION	<ul style="list-style-type: none"> HIGHLY IRREGULAR CLIMB "UPWIND"

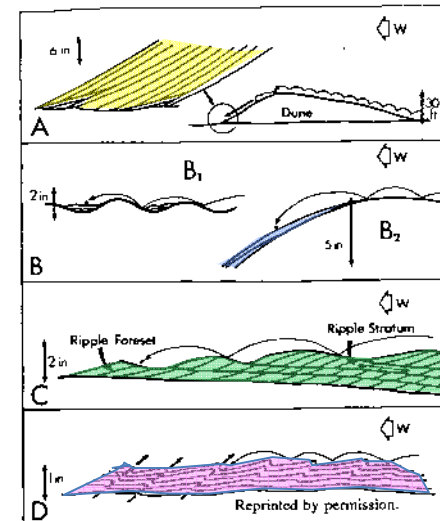
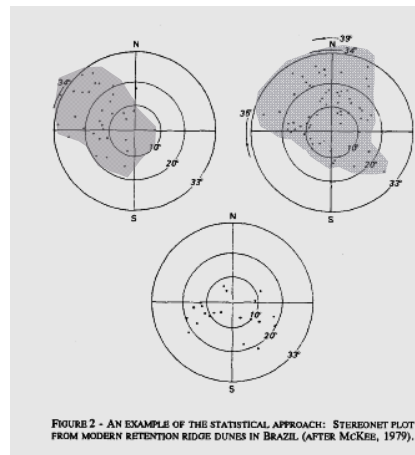


FIGURE 6 - PRIMARY EOLIAN STRATA AND ORIGINS. A: AVALANCHE, B: GRAINFALL, C: RIPPLE, D: ADHESION STRATA. BOTH FIG. 5 AND 6 AFTER FRYBERGER, ET AL., 1983.

After Fryberger, Krystinik and Schenk, 1991

8. Modern and Ancient analogues: *olian crossbedding within bedforms*

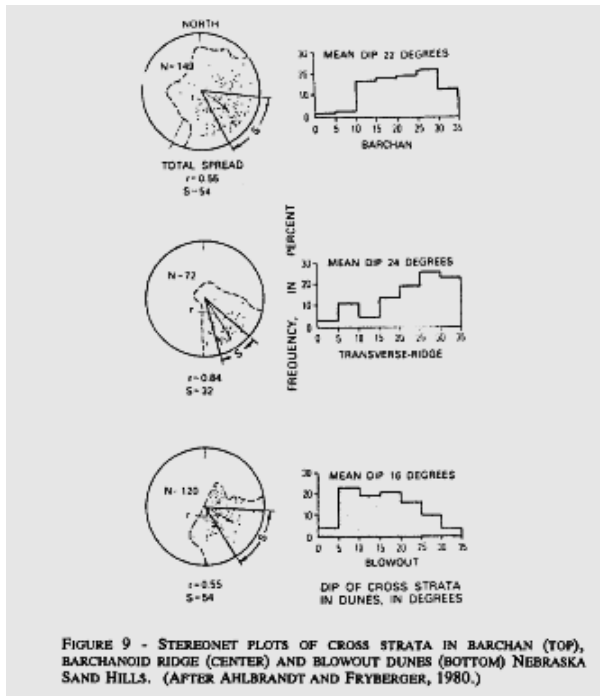


FIGURE 9 - STERONET PLOTS OF CROSS STRATA IN BARCHAN (TOP), BARCHANOID RIDGE (CENTER) AND BLOWOUT DUNES (BOTTOM) NEBRASKA SAND HILLS. (AFTER AHLBRANDT AND FRYBERGER, 1980.)

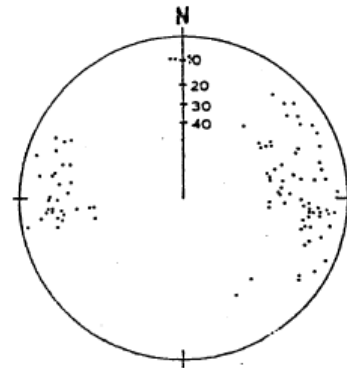


FIGURE 11 - STERONET PLOT OF CROSSBEDDING AZIMUTHS IN A STAR DUNE, GREAT SAND DUNES, COLORADO. AFTER ANDREWS, (1981).

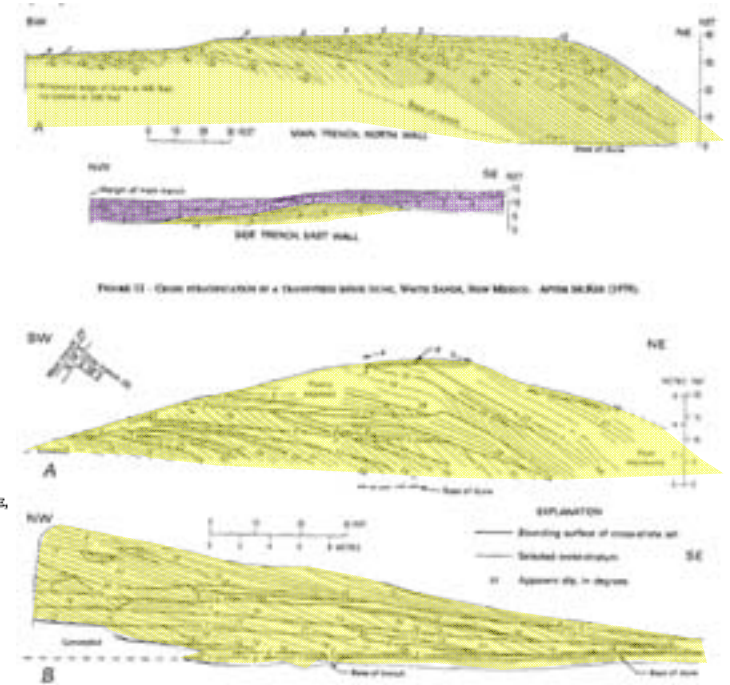


FIGURE 12 - CROSS STRATIFICATION OF A TRANSVERSE SAND DUNE, WHITE SANDS, NEW MEXICO. AFTER MEGAL (1976).

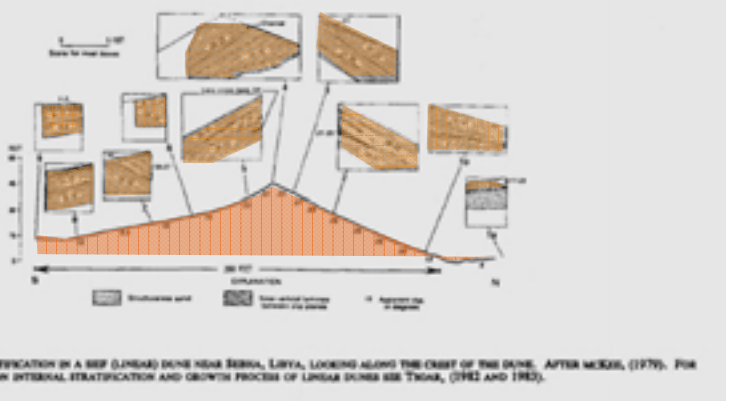


FIGURE 13 - CROSS STRATIFICATION IN A SEIF (LINEAR) DUNE NEAR BERNA, LIBYA, LOOKING ALONG THE CREST OF THE DUNE. AFTER MEGAL (1976). FOR FURTHER INFORMATION ON INTERNAL STRATIFICATION AND GROWTH PROCESSES OF LINEAR DUNES SEE THOMAS, (1982 AND 1983).

48

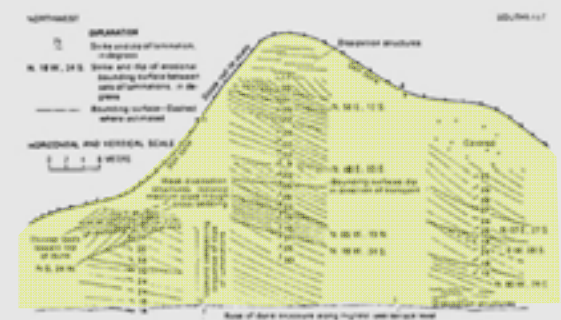
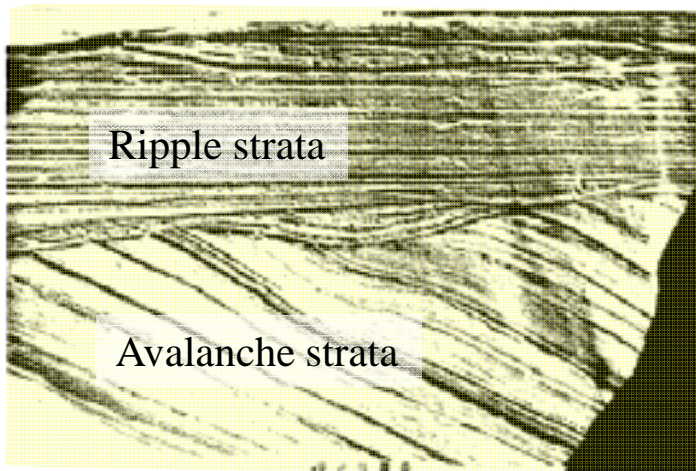


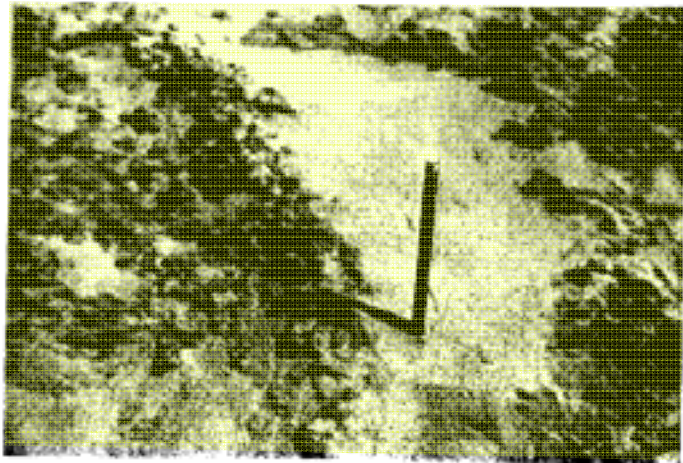
FIGURE 14 - EXPOSURE IN THE SIDE OF A LARGE BARCHANOID DUNE AT MERRITT RIDGEVIEW, NEBRASKA SAND HILLS. AFTER AHLBRANDT AND FRYBERGER, (1980).

After Fryberger, Krystinik and Schenk, 1991

8. Modern and Ancient analogues: *Crossbedding within dunes, salt ridge structures*

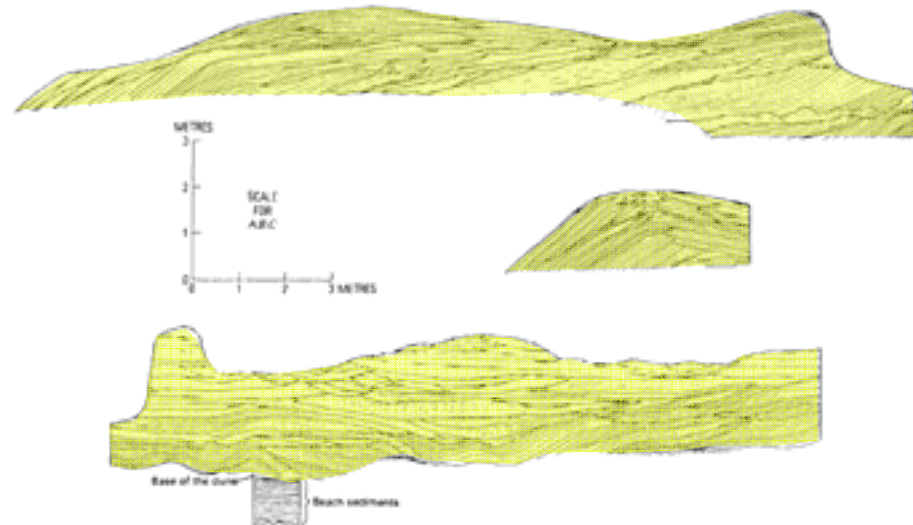


Trench in a barchan dune in Saudi Arabia. Which way did the wind blow?

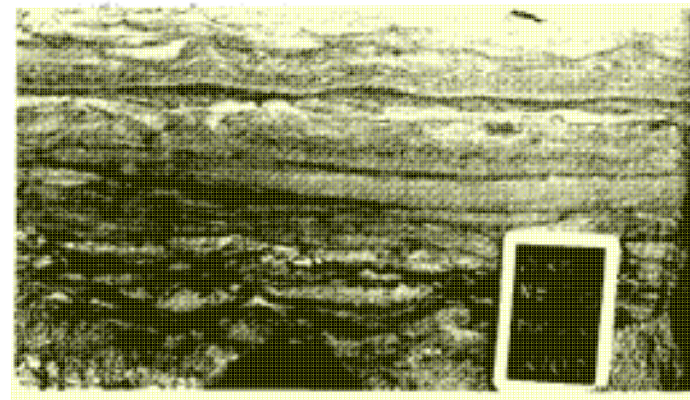


Bumpy salt ridge structure and light sand infill by wind, Saudi Arabia

After Fryberger, Krystinik and Schenk, 1991

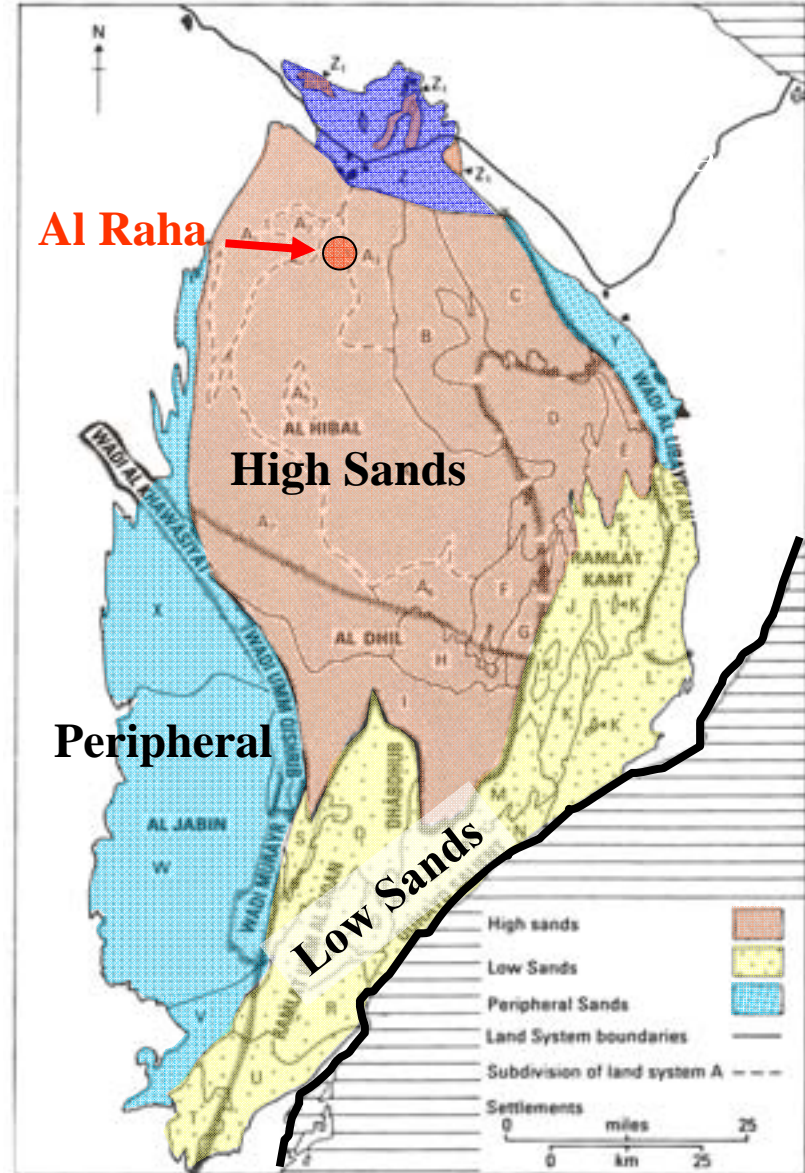
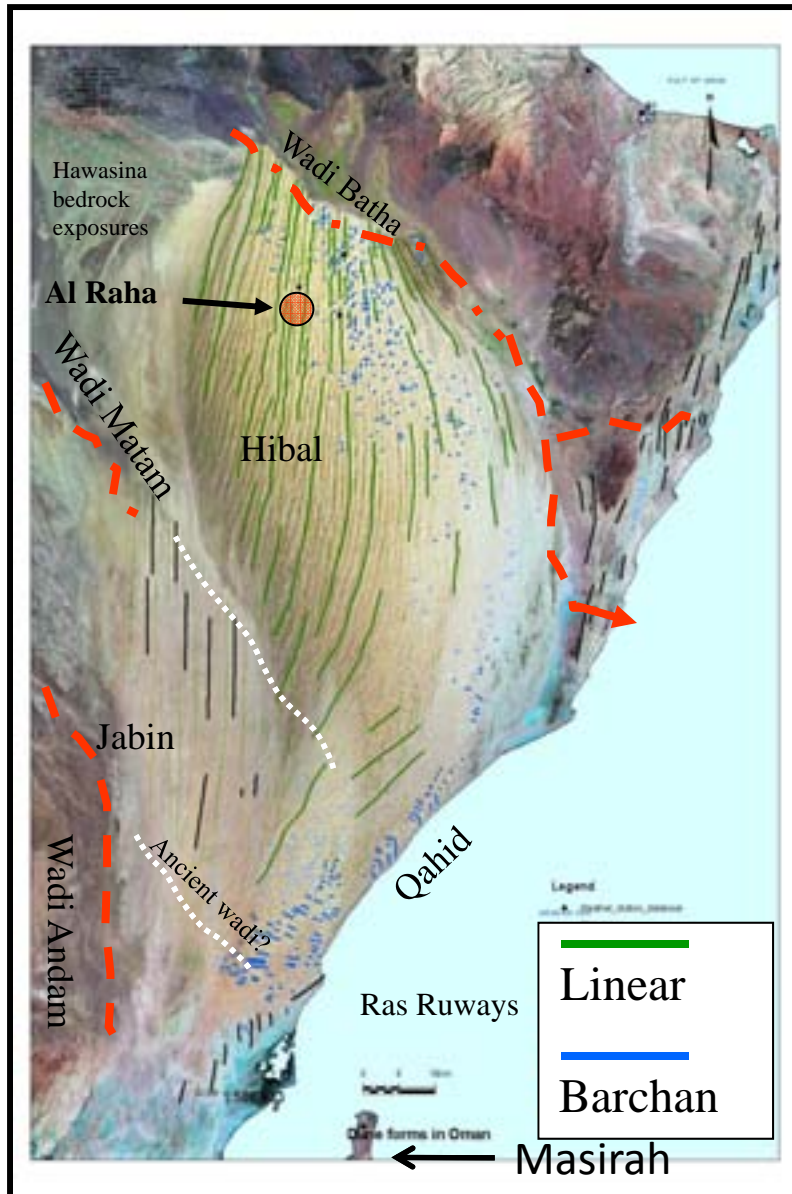


Stratification in a coastal retention ridge, Brazil, after Bigarella (In McKee, 1979)



Eolian sabkha deposit, Saudi Arabia. Note mix of salt ridge structures and dry eolian ripple strata.

8. Modern and Ancient analogues: Wahiba Sands, Oman. Dune facies distribution

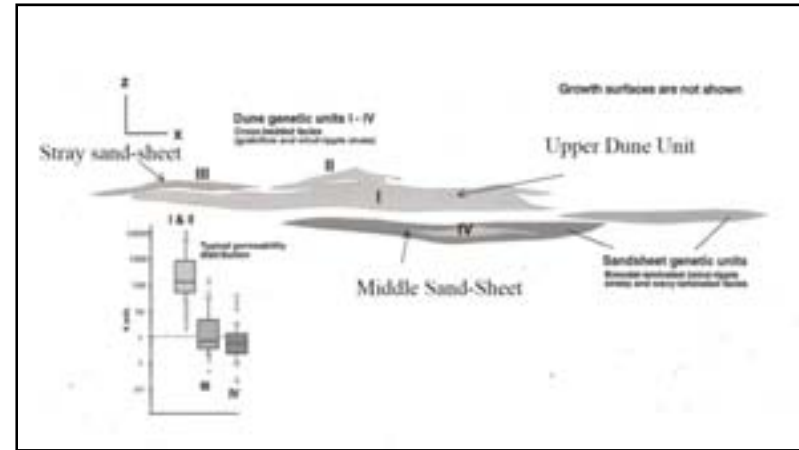


Aeolian dunes and sand terrains of the Wahibas: A, Satellite image of the Wahibas with analysis. B, Land systems in the Wahiba region, (after Jones K.D.C, et al., 1988).

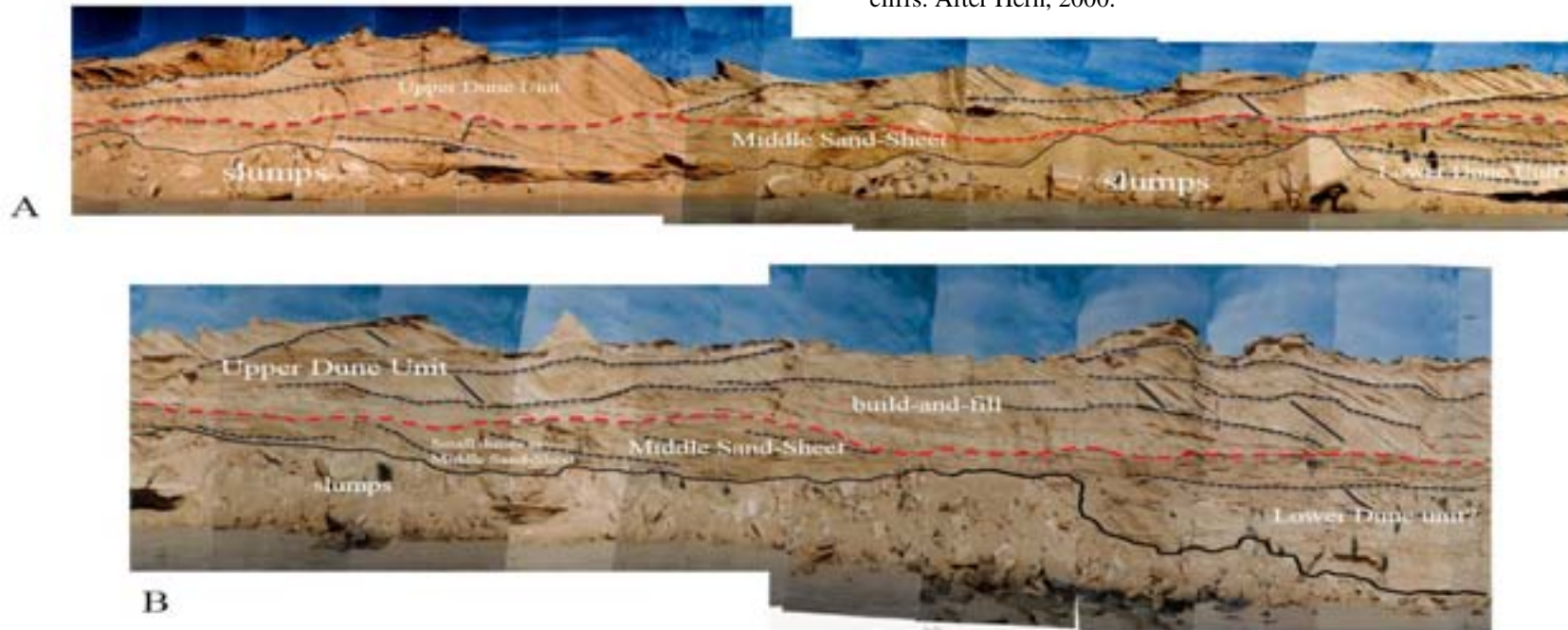
8. Modern and Ancient analogues: *Large scale genetic units in outcrop*

Lithified outcrops of the Late Pleistocene-Recent Wahiba Sands along coastal cliffs reveal the true potential complexity of eolian reservoirs at large and small scale.

Outcrop images and all flow analyses diagrams after Hern, 2000; and Fryberger, Hern and Glennie, 2010

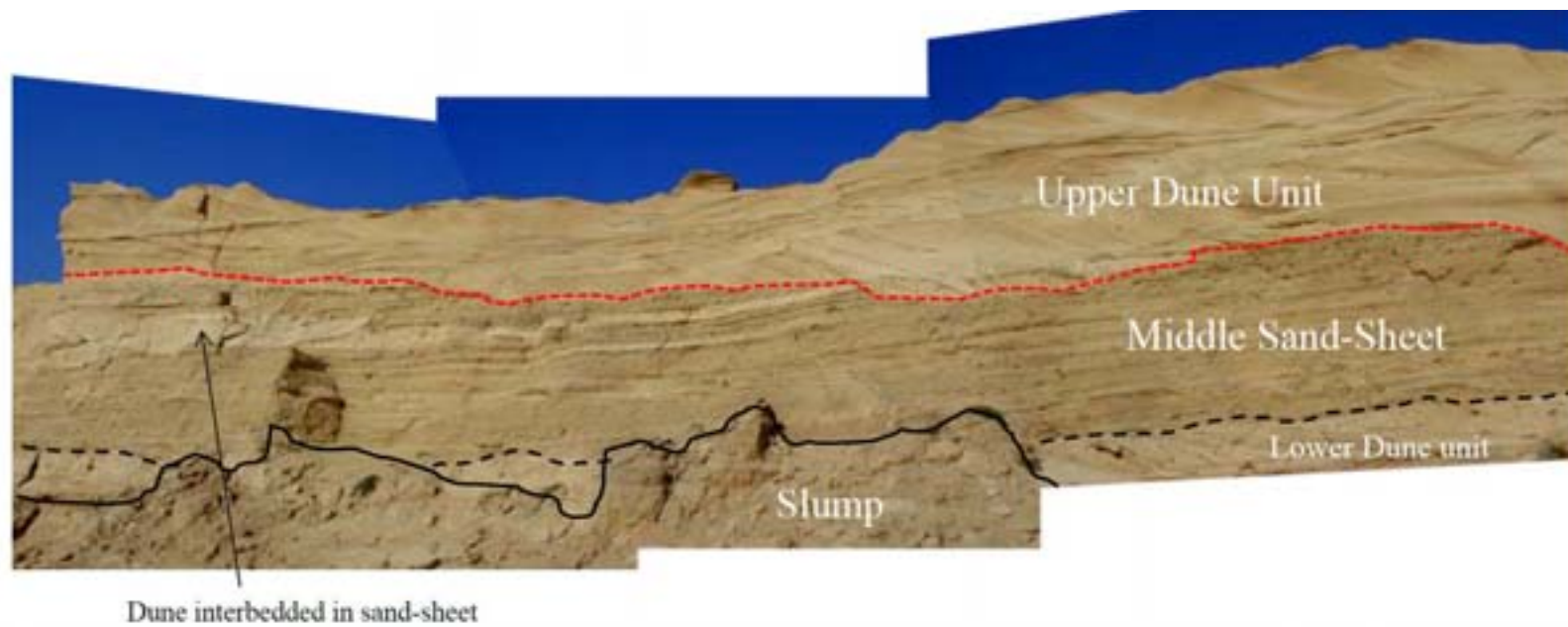
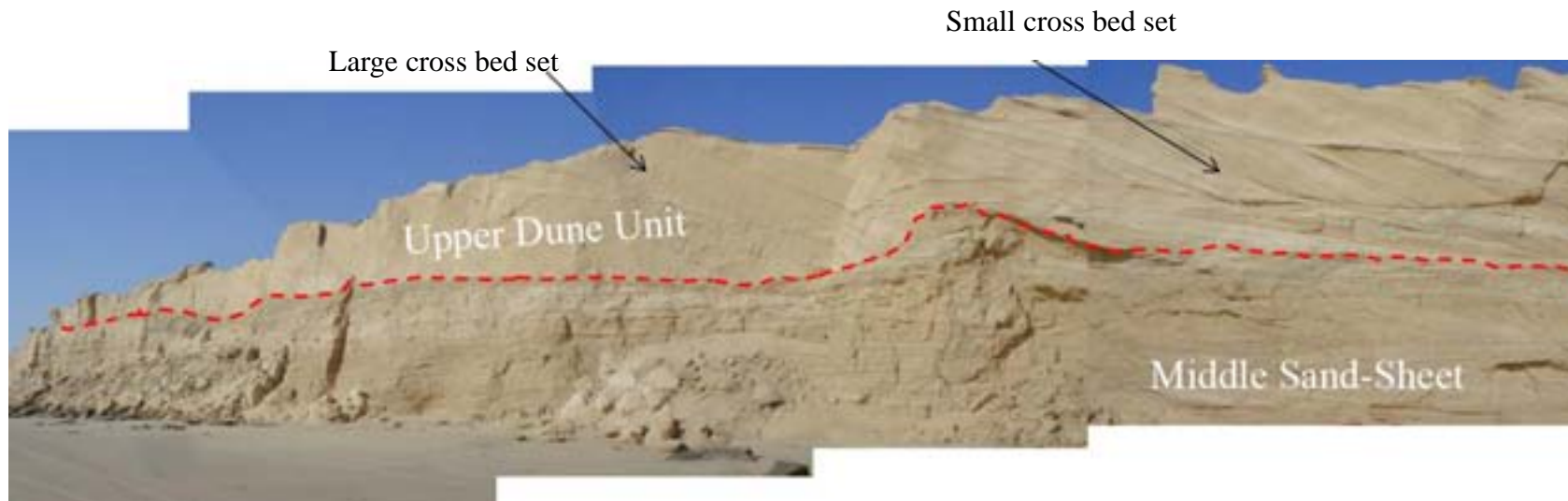


Schematic breakdown of major genetic units on the Ras Ruways (Qahid) cliffs. After Hern, 2000.



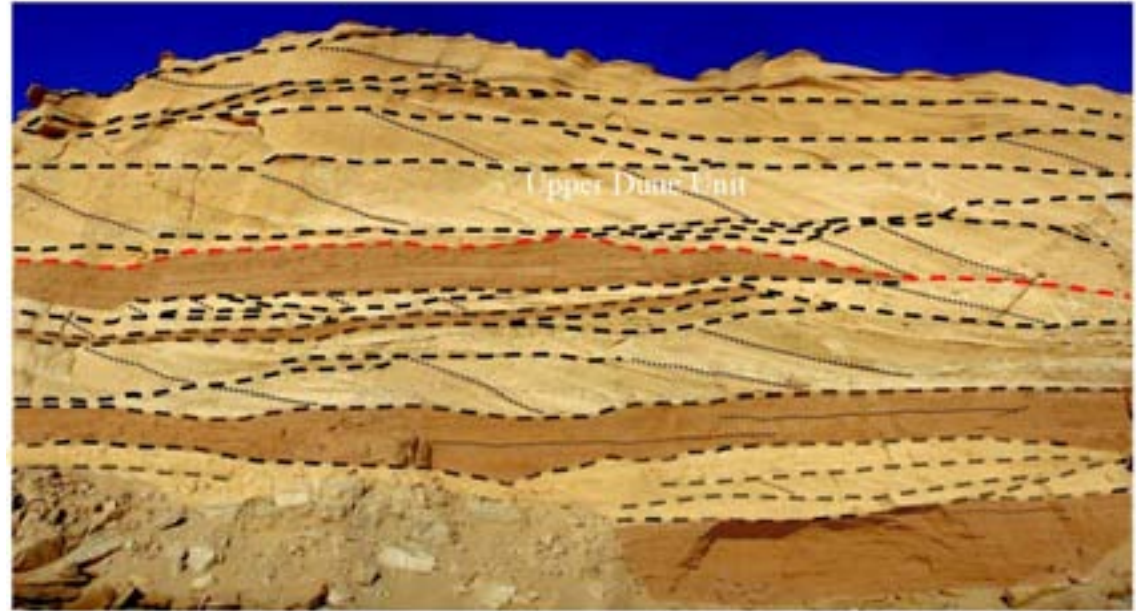
Outcrops of the Al Qahid unit of the Wahiba Sands north of Ras Ruways. A, climbing dunes in the Upper Dune Unit. B, build-and-fill in the Upper Dune Unit.

8. Modern and Ancient analogues: *Large scale eolian reservoir units in SE Wahibas*



8. Modern and Ancient analogues: *Intermediate scale genetic units in outcrop*

Wahiba Sands SE coast, lithified carbonate and quartz eolian dunes



Detail view of outcrop near figure 31 showing small-scale intercalation of sand-sheet (light and dark brown shading) and aeolian dune sands. Bold, mostly flattish dashed lines show stacking surface between bedforms and aeolian facies groups. Lower-rank growth surfaces shown by dotted lines. Major stacking surface between Upper Dune Unit and Middle Sand-Sheet is shown by red dashed line. Sand-sheet deposits were probably common in the Upper Dune Unit during early stages of deposition



The basic arrangement of the Upper and Lower Dune Units and the Middle Sand-Sheet Unit near Ras Ruways. The Middle Sand-Sheet is bioturbated beneath the very low-rank erosional bounding surface atop the sand-sheet. Note intercalation of sand-sheet and Upper Dune Unit. Lower bounding surface of the Middle Sand-Sheet is erosional. This image clearly shows the common interbedding of sand-sheet deposits in the Upper Dune Unit (shaded brown), and the dune sands in the Middle Sand-Sheet (shaded yellow). Stacking surfaces in the Upper Dune Unit of bedforms or facies shown by green lines. Growth surfaces representing alternate deposition and erosion of portions of a migrating dune slipface are shown in blue. Red lines show dips of primary aeolian ripple or avalanche strata.

8. Modern and Ancient analogues: *Intermediate scale genetic units in outcrop*

Image on right from Hern, 2000

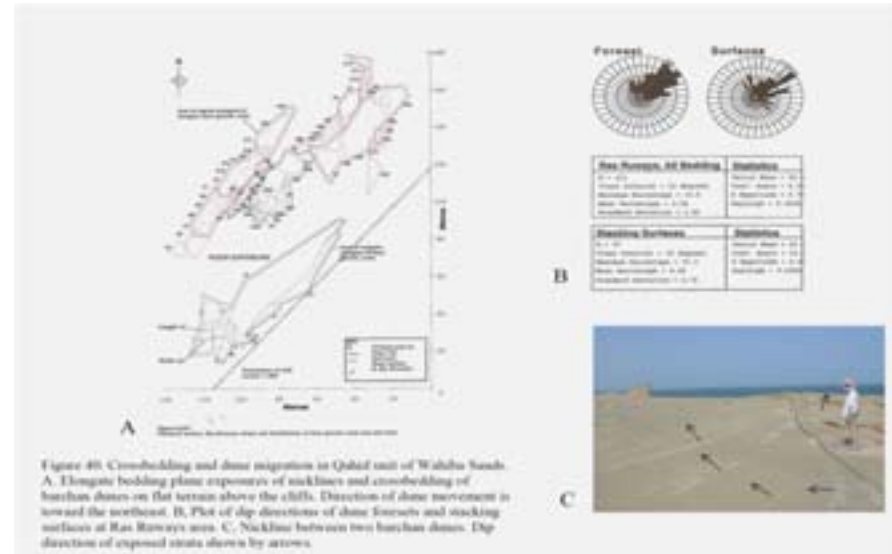
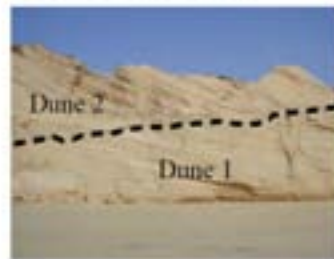


Figure 40. Crossbedding and dune migration in Qatuf unit of Wahiba Sands. A. Elongate bedding plane exposures of necklines and crossbedding of barhan dunes on flat terrain above the cliffs. Direction of dune movement is toward the northeast. B. Plot of dip directions of dune foresets and stacking surfaces at Ras Rarway's area. C. Neckline between two barhan dunes. Dip direction of depositional strata shown by arrows.



Build-and-fill in aeolian Wahiba Sands of the Upper Dune Unit south of Ras Rarway's. A. Rapid growth of a dune is followed to right by infill of accommodation space by smaller sets of crossbeds. These may represent a different style of dune advance, or cross-drift of sand or deposition by unrelated bedforms. Outcrop is about 15 metres high. B. Growth of Dune 1 has caused Dune 2 to climb at unusually steep angle as it filled accommodation space created upwind by Dune 1. Outcrop is about 6 metres high.



Upper Dune Unit



Dunes within the Middle Sand-Sheet. A. Three groups of mixed small dunes and ripple strata of sand-sheet separated by stacking surfaces (dashed lines) is laterally equivalent to, and roughly the same age as the main "sand-sheet". B. Closer view of dune crossbedding in A. Lighter unit (arrow) stands out in relief due to slightly better calcite cementation than sand-sheet unit above. Note biomaturation. Blue rectangle in "A" shows area of image B.

8. Modern and Ancient analogues: *Small scale genetic units in outcrop*



A

Above, and right: Eolian ripple laminations and vertical burrows, Ras Ruways area, Oman



B



C

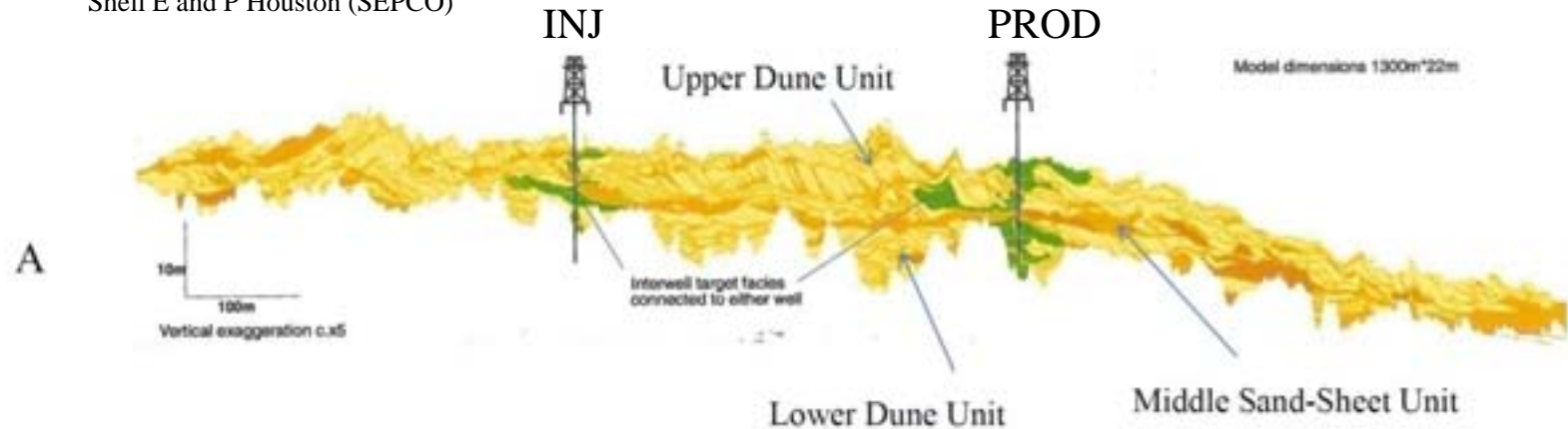
Bioturbation in the aeolian deposits, mainly the sand-sheets. A, Vertical insect burrows in ripple strata of the Middle Sand-Sheet. B, Burrows and contorted strata in Middle Sand-Sheet. C, Upturned strata associated with vegetative growth in Middle Sand-Sheet, black dashed lines show position of ancient plant rhizomes, white lines show distortion of sand sheet bedding produced by the plant. D, Insect trail on slipface deposits, Upper Dune Unit.



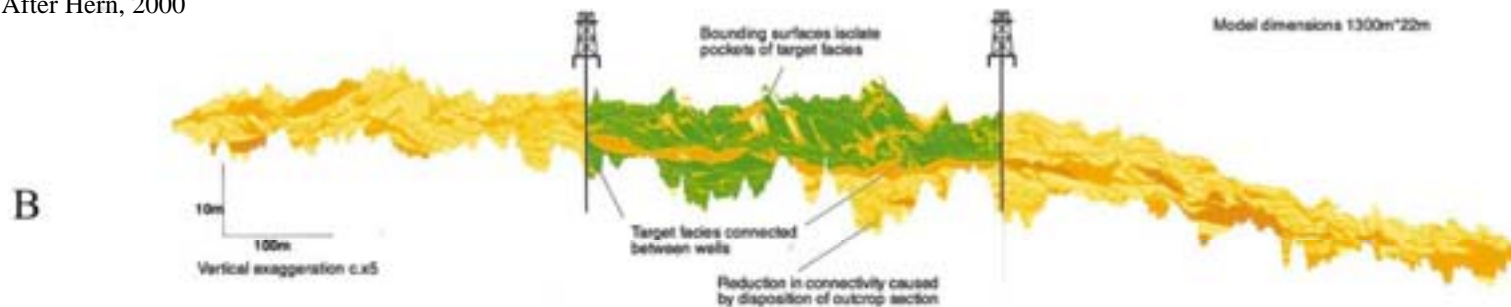
D

8. Modern and Ancient analogues: *Petroleum production model*

Injector-Producer model based on Al Qahid outcrops along Coastal Wahiba Sands, Oman. Model courtesy of Caroline Hern, Shell E and P Houston (SEPCO)



After Hern, 2000



The Qahid outcrops of the Wahiba Sands (lithified) considered as aeolian petroleum reservoirs. A, Severe isolation of two producing wells, and inefficiency when obstruction caused by small bounding surfaces and primary strata are considered. The result is limited sweep of the aeolian reservoir. B, Sweep diagram near two wells, one of which is an injector, the other a producer when only the major genetic units are considered as flow barriers. This results in moderately good sweep, although it is possible to observe some significant unswept areas between the two wells – for example within the crossbedding and two units isolated by the “unconformity” produced by the exposure pattern seen on outcrop. Green shows swept areas, yellow and orange show unswept areas.

8. Modern and Ancient analogues for eolian reservoirs: *Petroleum reservoir data and reservoir model*

Mark A. Chandler et al

665

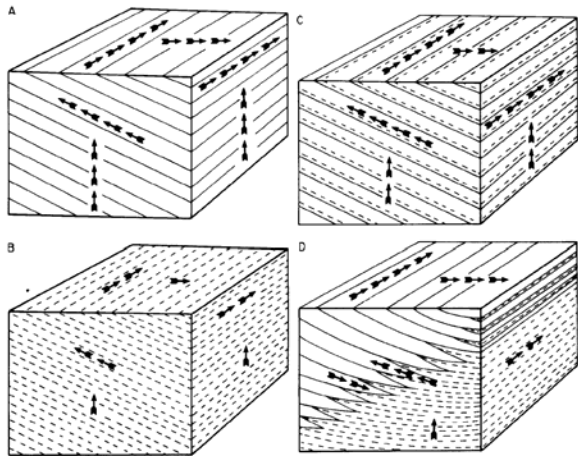


Figure 3—Common styles of cross-strata in Page Sandstone. Directional permeability indicated by arrows; more arrows denote higher potential flow. (A) Grain-flow set. (B) Wind-ripple set. (C) Interlaminated grain-flow and wind-ripple set. (D) Grain-flow foresets toeing into wind-ripple bottomsets.

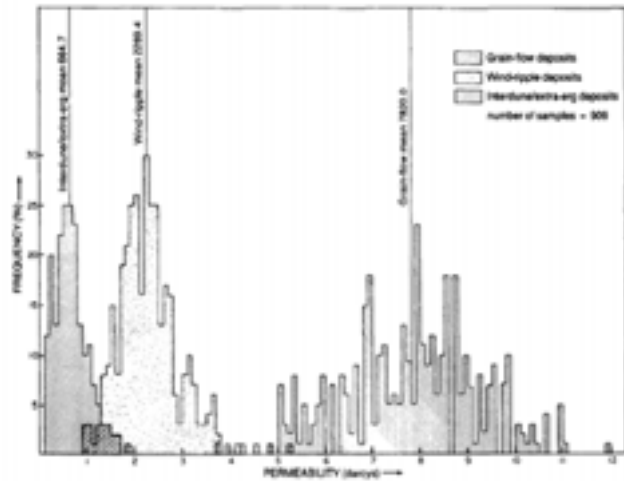
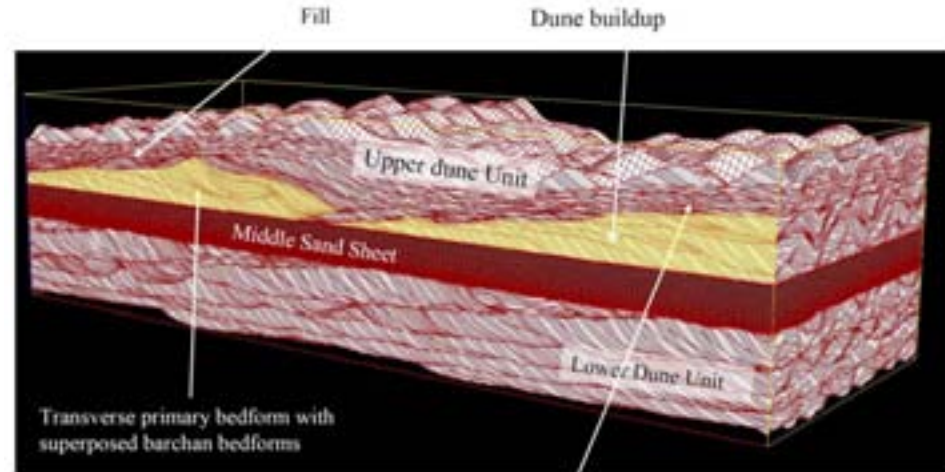


Figure 4—Histogram showing Page Sandstone permeability data. See discussion in text.

A. Preferred flow at small (laminar) scale predicted from minipermeameter measurements in Jurassic Entrada Sandstone. Minipermeameter data from outcrop. After Chandler, et al 1989



Figures above and below after Hern, 2000; and Fryberger, Hern and Glennie, 2010

Carapace of low effective permeability interval resulting from migration & infill of geomorphic accommodation space by smaller, faster moving bedforms

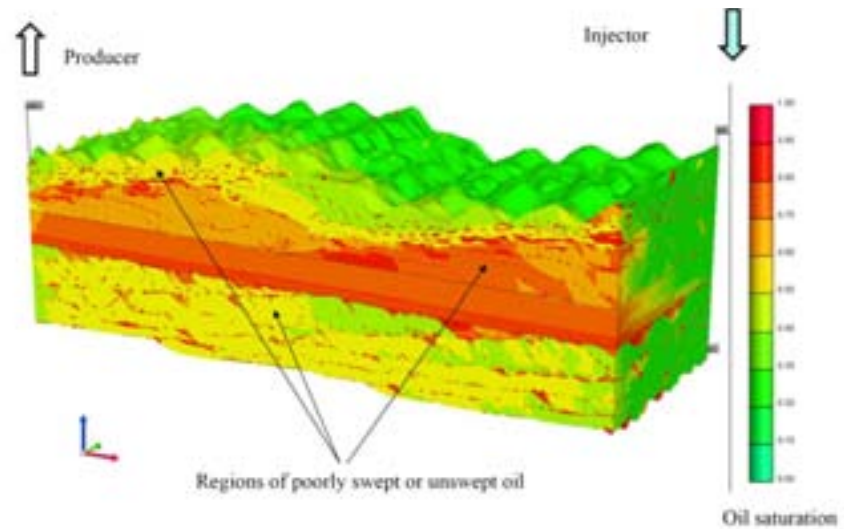


Figure 4B. The 3-dimensional Aulhus reservoir flow simulation, Ran Raways outcrops

8. Modern and Ancient analogues for eolian reservoirs: *Minipermeameter data and upscaling steps*

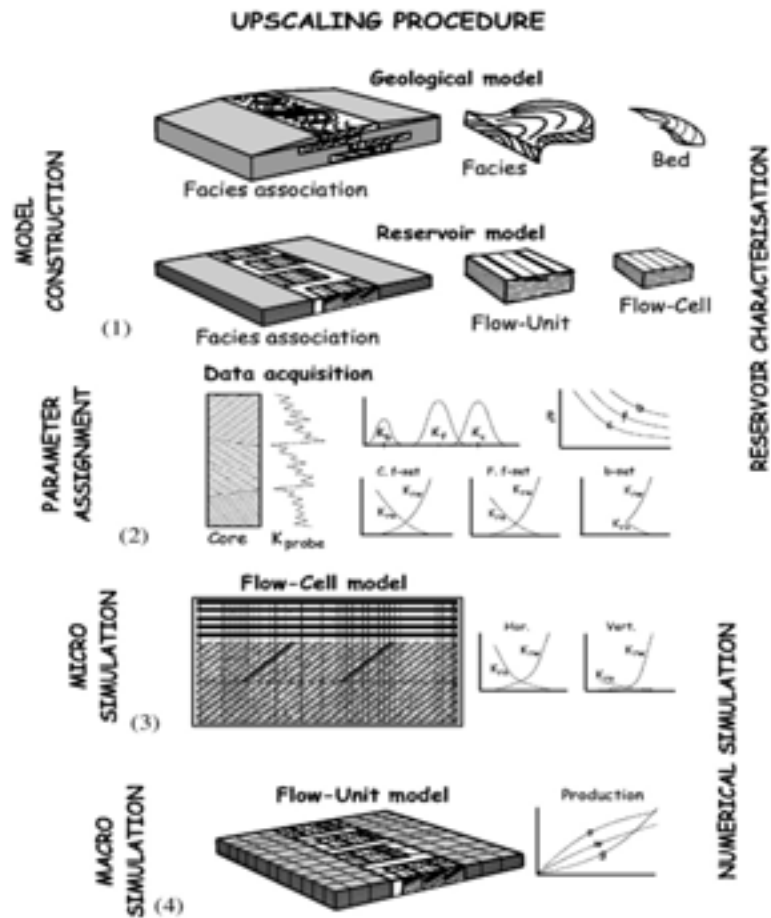


Fig. 1. Schematic representation of the four-step upscaling procedure of this work. Step 1: Model construction, consisting of geological and reservoir model and assignment of its elements. Step 2: Parameter assignment, consisting of permeability sampling, data analysis, and calculation of relative permeability and capillary pressure. Step 3: Micro-simulation, consisting of numerical flow simulation on all flow cell models of the reservoir, yielding effective 1- and 2-phase permeabilities, and capillary pressures. Step 4: Macro simulation consisting of numerical flow simulation on the entire reservoir, yielding production history. Steps 1 and 2 form reservoir characterisation. Steps 3 and 4 form numerical flow simulation. K_c , K_l , K_b are permeabilities of coarse-, fine foreset, and bottomset, resp. K_{co} , K_{fo} are relative permeabilities of oil and water, resp. C, F, B stand for coarse-, fine foreset and bottomset.

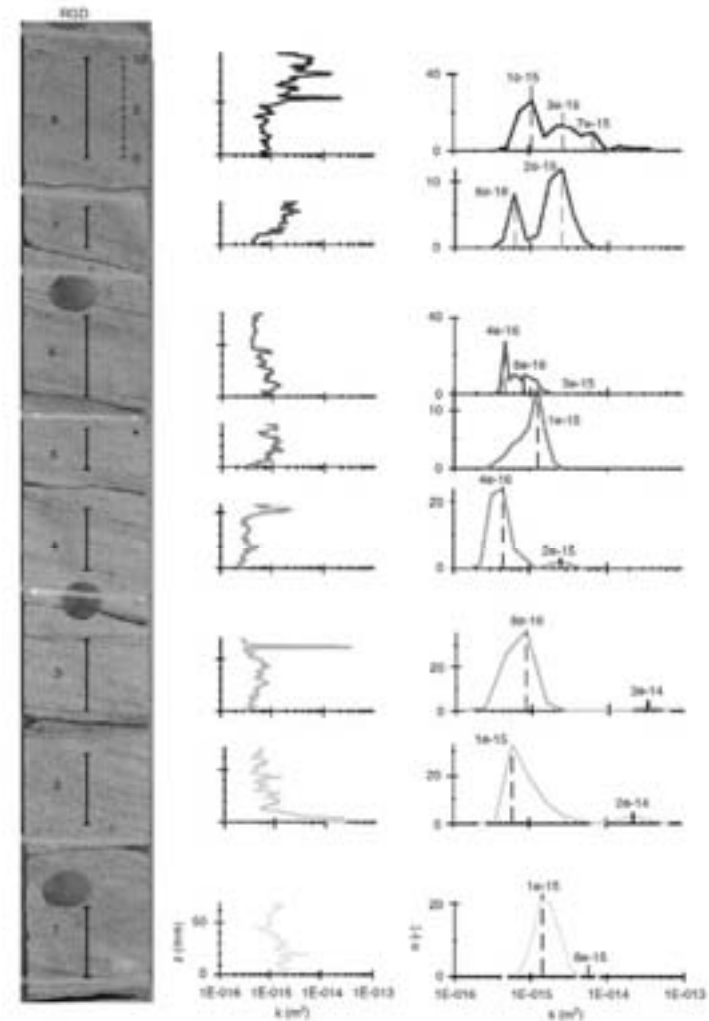
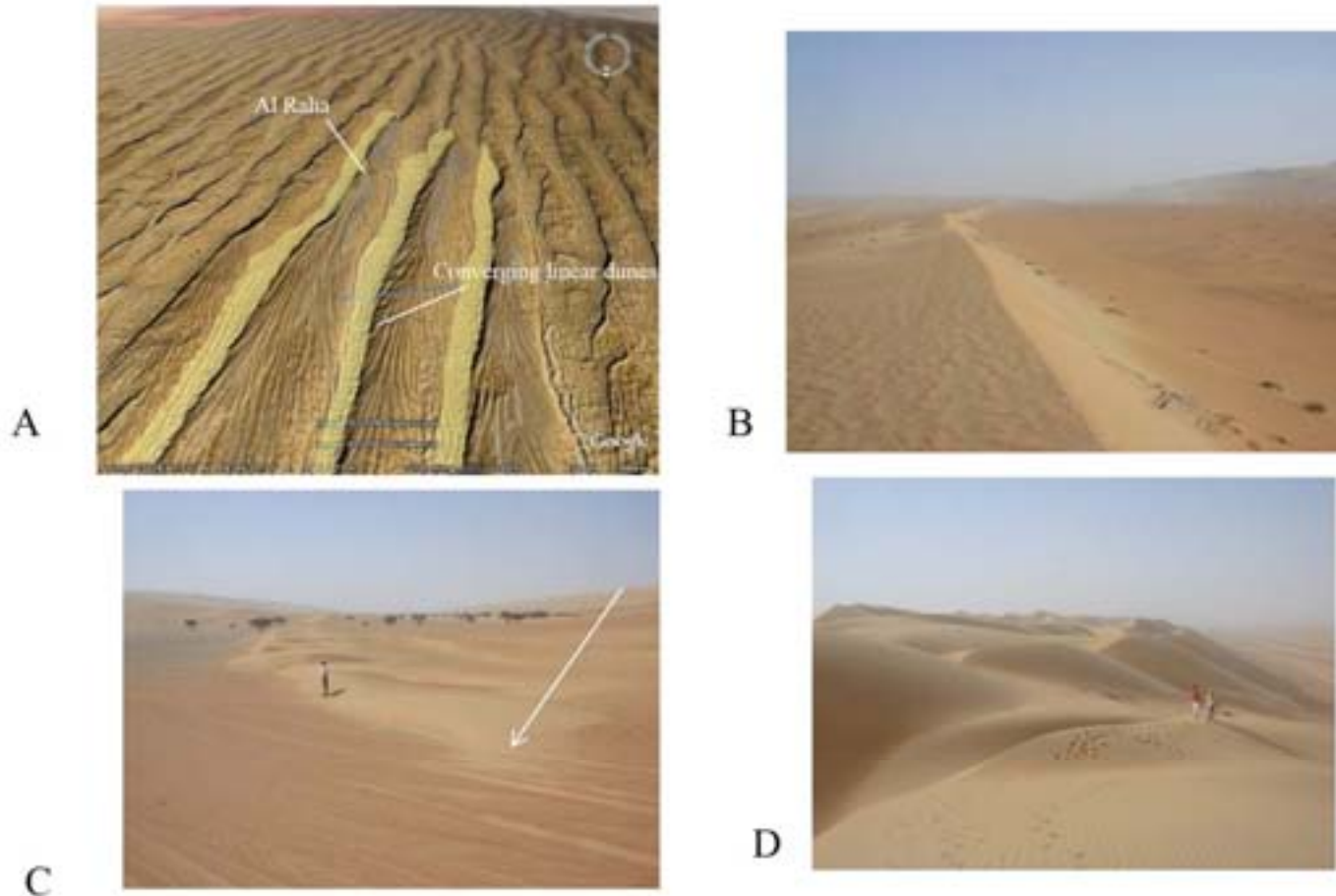


Fig. 10. Permeability curves from core RGD. Curves show different values, contrasts and trends and PWFs show different modes and shapes, ranging from unimodal symmetrical to skewed and from bimodal to trimodal. Permeability covers two orders of magnitude. Numbers indicate core sections, normally separated along bottomsets. Black lines indicate sample profiles, sample spacing is 1 cm.

Laminar scale permeability variation, and upscaling procedures

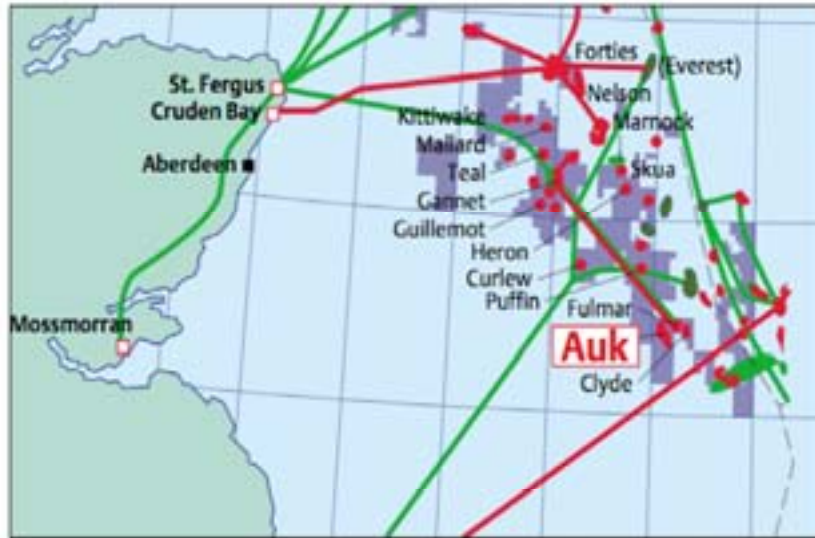
8. Modern and Ancient analogues for eolian reservoirs: *Linear dunes of the Wahiba Sands*



Geomorphology of the secondary bedforms of the linear megadunes. A. In the current wind regime small linear dunes are growing over and into the megadunes, adding volume, an active process we observed on the ground. Wind microenvironments created by megadunes in some places causes linear dunes to converge, as in noted portion of this image. View to south, image courtesy of Google Earth. Yellow shading shows higher parts of several megadunes to assist reader. B. View of a small linear dune just north of Al Raha, slipface has grown on the east side of dune due to sandstorm from the west. View to north. C. Growth of small linear dunes occurs from extension of sand tongues, sometimes as arms of barchanoid elements formed during storms View to south. D. Barchanoid ridge dunes developed atop one of the linear megadunes near Al Raha. In winter, slipfaces commonly flip towards the east in response to relatively weak northwesterly shamals. View to south toward Al Raha, which is just out of sight in distance.

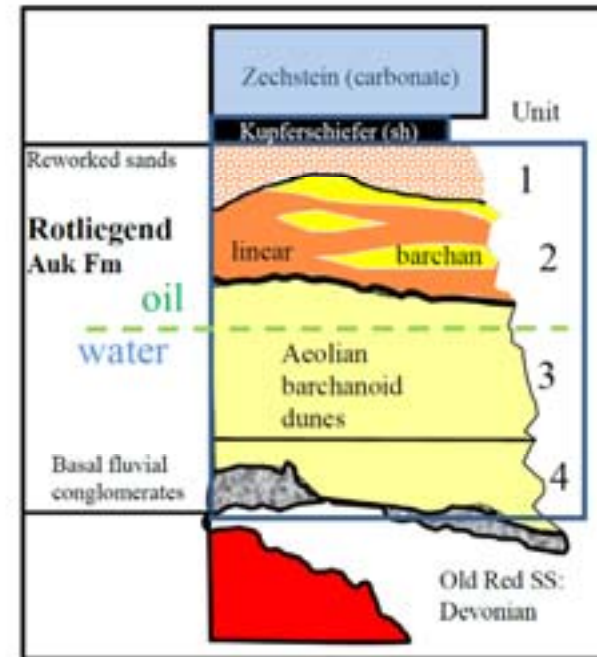
8. Modern and Ancient analogues: Auk Field, Northern North Sea

Location and stratigraphic column, Auk Field



A

After Trewin, Fryberger and Kreutz, 2003

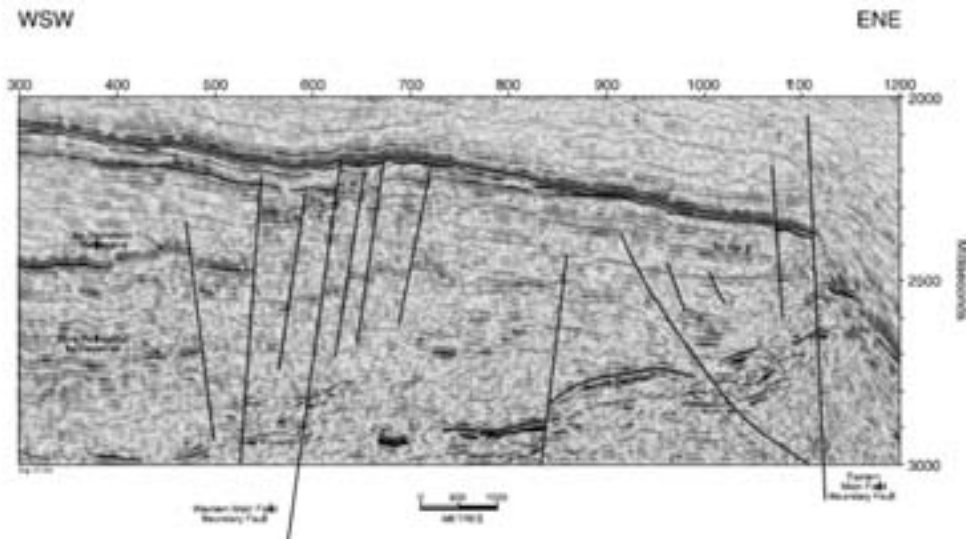


B

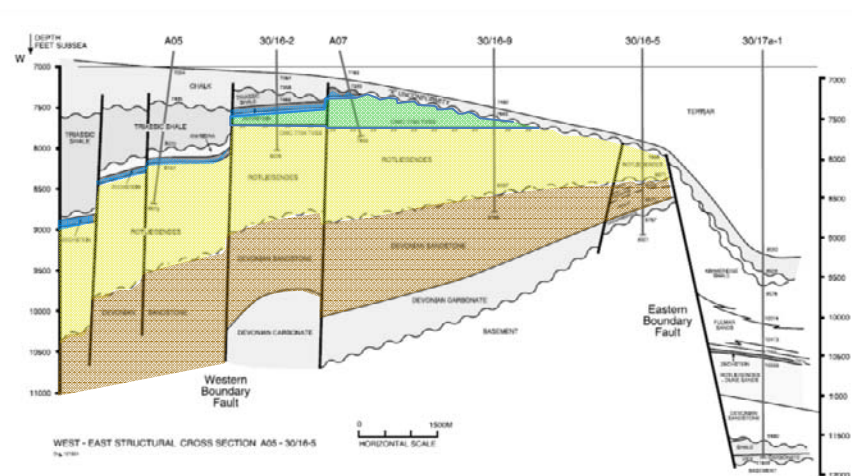
Map and cross section showing location and stratigraphy of Auk Permian Rotliegend oil field. A, Auk is located in the Northern Permian Basin of the UK. Oil is sourced from Kimmeridge (Cretaceous) shales downfaulted below the Rotliegend on the northeast side of the field. On the stratigraphic column, linear megadunes in unit 2 are suggested by the orange colour. The yellow suggests the infill of the linear megadunes by barchanoid dunes reworking them in a manner similar to the northern Wahibas. In this field, the (yellow) barchanoid dunes contain most of the oil and the best reservoir properties, while the linear dunes, mainly comprising poorly-sorted ripple strata from the preserved flanks are poor to non-reservoir. Oil-water contact is very generalized but expresses the overall situation in higher structural positions within the field.

8. Modern and Ancient analogues: *Auk Field, UK North Sea seismic and map data*

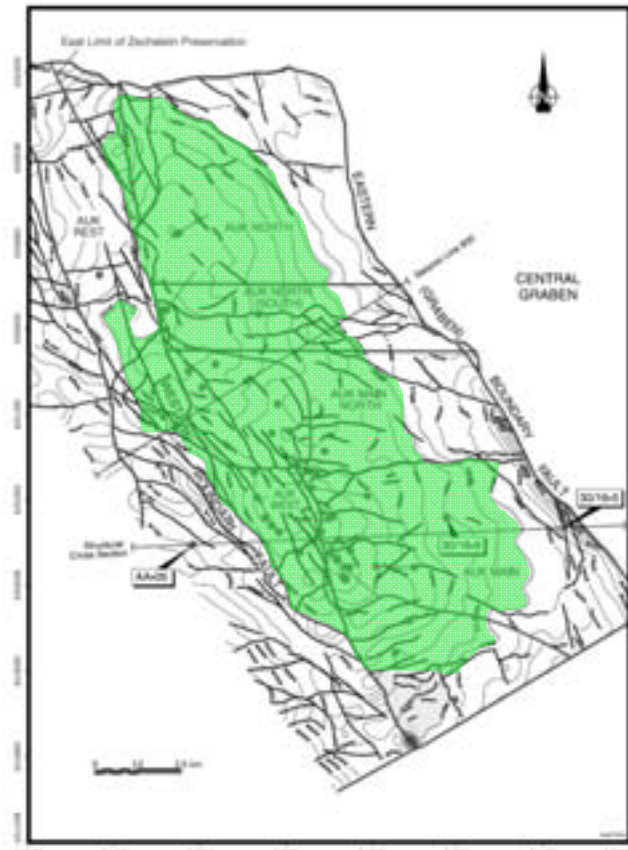
Auk field eolian oil/gas reservoir, UK North Sea



Seismic cross section in SW-NE direction through Auk Main North block.



Geological cross section in W-E direction through Auk Main block and into the Central North Sea Graben, illustrating the trapping of hydrocarbons to the west against Aptian shales.



Top Rotliegend structure map and well locations, Auk field. The Zechstein is only preserved in the west part of the field, towards the east Early Cretaceous erosion has removed all of the Zechstein, and cut into the Rotliegend reservoir.

8. Modern and Ancient: Auk Field, UK North Sea

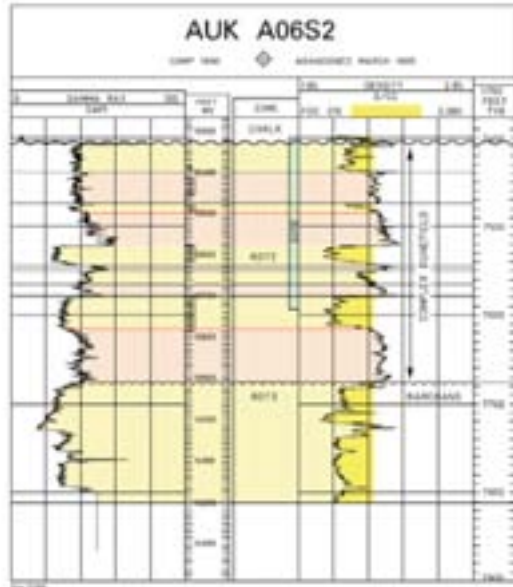
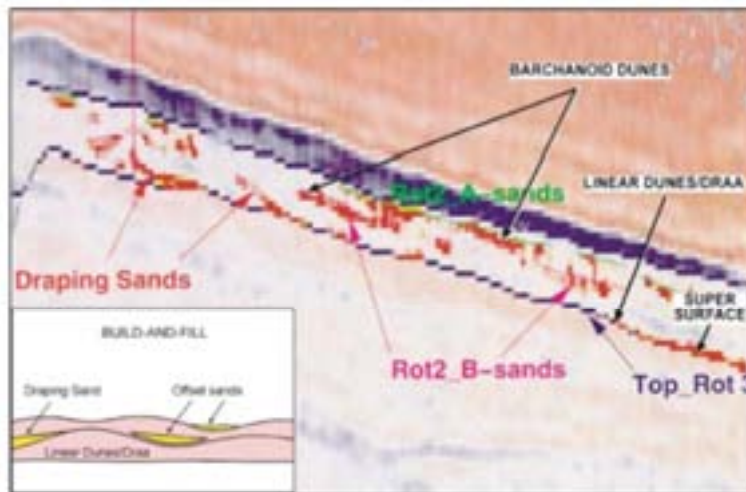


Fig. 7. Typelog for the Rotliegend unit 2 reservoir and Rotliegend unit 3 aquifer, yellow indicates net reservoir whilst orange-brown indicates waste zones. The Rotliegend unit 1 and the Zechstein is eroded in this well.



Seismic panel showing the build-and-fill pattern of porous barchanoid dune sandstones in the Rotliegend (red colours) in-filling between poor quality linear dune sandstones (pale colours).

After Trewin, Fryberger and Kreutz, 2003

Fryberger, Jones and Johnson, 2014



Satellite image of the northern Wahibas with analysis of bedforms. Green lines show positions of some small linear dunes. Black lines show linear megadunes, blue lines show trends of slipfaces of barchanoid dunes that are reworking the linear megadunes. Interdune studied in detail (trenches) indicated by white arrow. Glennie (2005) reported dates in dune sand above gravel in a well at Hawiyya of 110 and 127K YBP. At the north end of the village wadi gravels interbedded with thin aeolian sand were dated at 10 K YBP in excavations for a new school.

8. Modern and Ancient analogues: *Auk Field geological model*

Modern analogue in Northern Wahibas, Oman

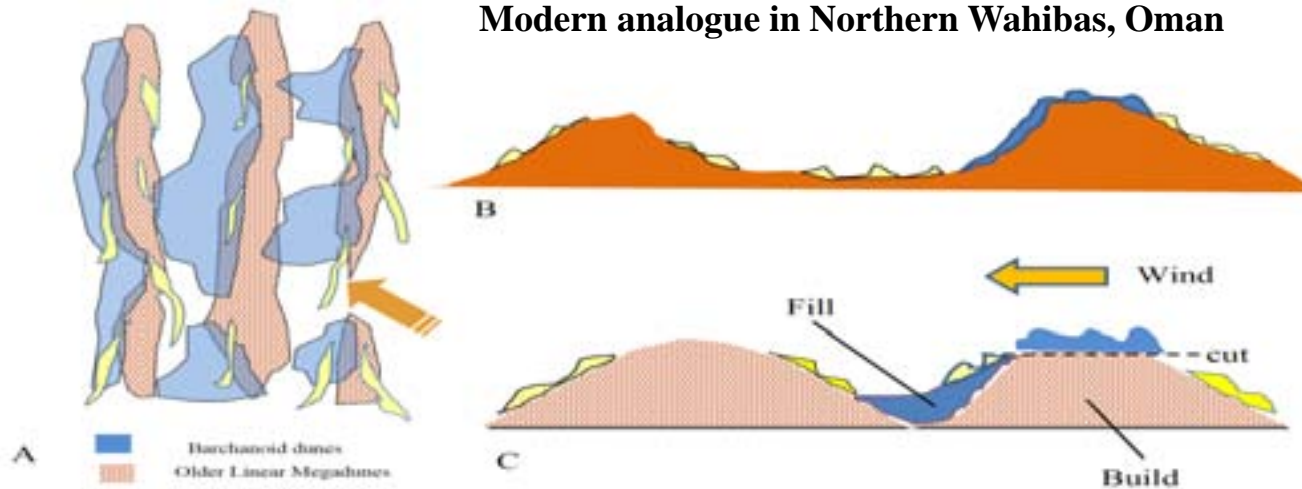


Figure 71. Cartoons illustrating the build-and-fill, as well as cut-and-fill processes we observed in the northern Wahiba linear megadunes. A, Reworking of linear megadunes occurs by rollover of tops through erosion of upwind side of dune followed by formation and migration to the slipface of small barchanoid dunes. The accommodation space created by the formation of the large megadunes is also filled by accretion of small linear bedforms to the linear megadune. Sand for these is supplied through regional migration of sand, mainly along interdunes, and by cannibalization of portions of the linear megadune. B, Reworking scenario when interdune is wide. C, Reworking scenario when interdune is narrower due to convergence of the larger dunes.

Ancient analogue along Moray Firth Coast, Scotland, Hopeman Sandstone

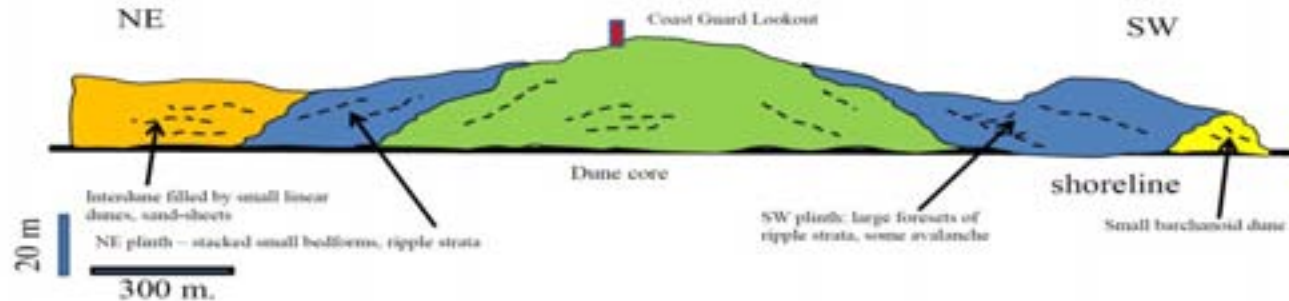


Figure 74. A three km outcrop of the Permian Hopeman Sandstone (Upper Rotliegend or perhaps younger Zechstien Equivalent) along the beach near Hopeman, Scotland, showing a preserved linear megadune. Most of the rock represented here consists of aeolian ripple strata with some stray sets of avalanche strata. Note build of the linear megadune followed by fill of accommodation space in interdune by small linear dunes and sand-sheets (orange colour). Although hard to show on a single A4 page, the megadune is asymmetric, with the southwest side built out farther from the dune core than the northeast side. View is toward the southeast, away from the ocean. From the senior author's sketchbook.

9. References Cited and Bibliography

- Agatston, R.S., 1954, *Pennsylvanian and lower Permian of northern and eastern Wyoming*, Bull Amer. Assoc. Petrol. Geol., vol. 38, pp. 508-83.
- Brady, F.H., 1931, *Minnelusa formation of Beulah district, northwestern Black Hills, Wyoming*, Bull. Amer. Assoc. Petrol. Geol., vol. 15, p. 183-188.
- Brady, F.H., 1958, *Evaporite deposits in the Minnelusa formation in the Sundance-Beulah area, Crook county, Wyoming*, Wyoming Geological Association Guidebook, 13 Annual Field Conference, p. 45-47.
- Chandler, M.A., Kocurek, G., Goggin, D.J. and Lake, L.W., 1989, *Effects of Stratigraphic Heterogeneity on Permeability in eolian Sandstone Sequence*, Page Sandstone, Northern Arizona, A.A.P.G. Bulletin, v. 73, no 5, p. 658-668.
- Condra, G.E., and Reed, E.C., 1940, *Correlation of the Carboniferous and Permian Horizons in the Black Hills and the Hartville uplift*, Guidebook 14th Annual Field Conference, *Western South Dakota and Eastern Wyoming*, Kansas Geological Society, p. 127-128 (abs.)
- Condra, G.E., Reed, E.C., and Scherer, L.J., 1940, *Correlations of the formations of the Laramie range, Hartville uplift, Black Hills, and western Nebraska*, Nebraska Geological Survey Bulletin 13, 52 pp.
- Foster, D. I., 1958, *Summary of the Stratigraphy of the Minnelusa Formation, Powder River Basin, Wyoming*, Wyoming Geological Association Guidebook 13th Annual Field Conference: Powder River Basin of Wyoming, p. 39-43 (with cross sections and maps).
- Frederick, J.B., Dean K.T., Fryberger, S.G. and Wilcox, T.D., 1995, *Donkey Creek North Minnelusa 3-D: Challenging Conventional Wisdom*, Rocky Mtn. Assoc. Geologists, High-Definition Seismic Guidebook-1995, Inden et al 1996
- Fryberger, S. G., 1979, *Dune forms and wind regime*, in E. D. McKee, ed., *A Study of Global Sand Seas: Geological Society Professional Papers*, Washington, US Government Printing Office, p. 137-169.
- Fryberger, S. G., Al-Sari, A.M. & Clisham, T.J., 1983, *Eolian dune, interdune, sand sheet and siliciclastic sabkha sediments of an offshore prograding sand sea, Dhahran Area, Saudi Arabia*: The American Association of Petroleum Geologists Bulletin, v. 67, p. 280-312

9. References Cited and Bibliography 9 (cont.)

Fryberger, S.G., 1984, *The Permian Upper Minnelusa Formation, Wyoming: Ancient example of an offshore-prograding sand sea with geomorphic, facies, and system-boundary traps for petroleum*, Wyoming Geol. Association 35th Annual Field Conference Guidebook, p. 241-271.

Fryberger, S.G., Hern, C.Y. and Glennie, K.W., 2010, *Wind regimes, sand transport and sedimentology of the Wahiba Sand Sea, Oman, with some implications for petroleum exploration and production*, PDO (Petroleum Development Oman) Exploration Report 630, 40 pp. + figures and maps.

Hern, C.Y., 2000, *Quantification of aeolian architecture and the potential impact on reservoir performance*, PhD thesis, Institute of Petroleum Engineering, Heriot-Watt University.

Jennings, T.V., 1959, *Faunal Zonation of the Minnelusa Formation, Black Hills, South Dakota*, Journal of Paleontology vol. 33, no. 6, p. 986-1000.

Jones, K.D.C. , Cooke, R.U. and Warren, A., 1988, *A terrain classification of the Wahiba Sands of Oman*, Journal of Oman Studies, v. 3, the Scientific Results of the Royal Geographical Society's Oman Wahiba Sands Project, 1985-1987, p. 19-32.

Love, J.D., Henbest, L.G. and Denson, N.M., 1953, *Stratigraphy and Paleontology of Paleozoic rocks, Hartville area, eastern Wyoming*, U.S. Geol. Survey Chart OC 44, Oil and Gas Investigation Series.

Maughan, E. K., 1967, *Eastern Wyoming, eastern Montana and the Dakotas*, **in** Mckee, E.D. and Oriel, S.S., eds., *Paleotectonic Investigations of the Permian System in the United States*; U.S. Geological Survey Professional Paper 515, p. 129-156.

Mikes, D., 2006, *Sampling procedure for small-scale heterogeneities (Crossbedding) for reservoir modelling*, Marine and Petroleum Geology, v. 23, p. 961-977.

Rascoe, B. and Baars, D.L. 1972, *Permian System*, in Atlas of the Rocky Mountain Region, R.M.A.G. Denver, p. 143-165.

Schenk, C.J., 1990, *Core Examples of eolian sandstone*, **in**: Fryberger, S.G., Krystinik, L.F., and Schenk, C.J.; *Modern and Ancient Eolian Deposits: Petroleum Exploration and Production*; Published by Rocky Mountain Section, S.E.P.M. 240 p.

9. References Cited and Bibliography (cont.)

Trewin, Fryberger and Kreutz, 2003, *The Auk Field, Block 30/16, UK North Sea*: in Gluyas, J.G. and Hichens, H.M. (eds), *United Kingdom oil and Gas Fields, Commemorative Millennium Volume*, Geological Society, London, Memoir, 20, 485-496.

Tromp, P. and TeSelle, R., 1984, *Casper Guernsey Reservoir to Newcastle*, in Goolsby and Morton, eds., *Field Trip Road Logs, The Permian and Pennsylvanian Geology of Wyoming*, WGA 35th Annual Field Conference, p. 410-420.

Tromp, P.L., 1981, *Stratigraphy and depositional environments of the "Leo Sands" of the Minnelusa formation, Wyoming and South Dakota*, MS Thesis, University of Wyoming, 69 p.

Trotter, J. F., 1984, *The Minnelusa Revisited*, in 35th Annual Field Conference Guidebook, *The Permian and Pennsylvanian Geology of Wyoming*, p. 127-151.

Weber, K.J., 1987, *Computation of initial well productivities in aeolian sandstone on the basis of a geological model, Leman Gas Field, U.K.*, Society of Economic Paleontologists and Mineralogists ((SEPM), Special Publication 40, *Reservoir Sedimentology*, p. 335-354.

Notes and sketches: page intentionally left blank

Notes and sketches: page intentionally left blank